Estimation of forest stand structure in Andean (agro)forests using 3D UAV remote sensing

Sergio Andrés Bolívar Santamaría

Trabajo de Grado para Optar al título de Magister en Biología

Director

Björn Reu

PhD en Ciencias Naturales

Universidad Industrial de Santander

Facultad de Ciencias

Escuela de Biología

Maestría en Biología

Bucaramanga

2020

Acknowledgements

First, I would like to thank all members of the socio-ecological landscape study group (PASOECO), especially my mentor and supervisor Dr. Björn Reu for this opportunity, all your encouragement, patience, and support. I am grateful to you for all your lessons and your dedication to the work of teaching and research in Colombia. Thank you for introducing me to the world of remote sensors and their contribution to conservation biology. I also appreciate the attention, advice, and support of Dra. Corina Buendía who always seeks to convey her vision that socio-ecological resilience can help us achieve sustainability. Thanks to Mateo Jaimes who was my partner and co-driver in our adventure with "kamikaze" (the fixed-wing UAV Mapper). Thank you for all your support on field work, without you I could not finish my work at this time, but not less important thanks for your friendship. Also, I want to thank Daniel Badillo for your friendship, support with accommodation, transportation, and so on during field work and flight missions. Thank you, Dani, for working for the knowledge and conservation of the birds of Santander. Other members of PASOECO from whom I thank and from whom I learned a lot for their exceptional skills are Tatiana Rodríguez, Erika Garcés y Kateryn Grimaldos, thank you for help to the construction of transdisciplinarity through your work with communities and decision makers. Thanks for your love and all your support girls, I am very lucky to know you.

I would like to thank to Yovanny Duran, Xaver Schenk, Valentin Fromm, Alwin Sämman, René Ardila, Hanna Penzlin, Luisa Saavedra and Mauricio Pabón, for your help on the hardest field work, but also for your smiles, knowledge and your excellent company. I am very grateful to all the producers and co-researchers of *Las Cruces.* Thank you very much for getting up every day to work, providing us nutritious and delicious food while taking care of nature, you are really

heroes. Thank you to FiNCO's initiative producers which really seek sustainability, resilience, and forest conservation. Thank you for my cup of coffee in the morning to Esmeralda Gualdrón, Carlos Buitrago and their family in *Los Laureles* farm, producers of the most delicious coffee that I have never tasted before. Thanks to Joaquín Blanco to share his knowledge of native plants and for his contribution to conservation tree species through the use. I want to thank Stphanie Angarita for being my English teacher and for carefully reviewing and improving English grammar in the document at the last minute; I appreciate a lot of what you do, sweetheart. Finally, I thank my parents, my sisters, and my family for all their love, care, support, home, food, life and all the bases that allowed me to get here. I love you.

"If I have seen further it is by standing on the shoulders of Giants."

Isaac Newton

Table of contents

Pág.

List of Tables

Pág.

List of Figures

Pág.

List of Appendices

Pág.

Glossary

AFS: Agroforestry systems.

AGB: Above-ground biomass.

CC: Canopy cover.

CHM: Canopy height model.

DSM: Digital surface model.

DTM: Digital terrain model.

D_mid: Density of midstory plants.

D_over: Density of trees in overstory.

H_mid: Mean height of plants in the midstory.

H_over: Mean height of trees in overstory.

H_sd_over: Standard deviation of heights in overstory.

LAI: Leaf area index.

Pcoa1: 1st principal coordinate axis, based on ordination with bird composition.

Pcoa2: 2nd principal coordinate axis, based on ordination with bird composition.

SfM point-clouds: Set of points with coordinates in the three axes (X, Y and Z), which represent the surface of terrain.

UAV: Unmanned Aerial Vehicle.

Resumen

Título: Estimación de la estructura forestal en agroforestales Andinos usando teledetección 3D con UAV [*]

Autor: Sergio Andrés Bolívar Santamaría[**]

Palabras Clave: Agroforestales, drones, teledetección, estructura del dosel, variables esenciales de la biodiversidad.

Descripción: Los sistemas agroforestales (AFS) son de gran importancia para la conservación de la biodiversidad fuera de las áreas protegidas. La composición de las plantas de cultivo y de sombra en los AFS proporciona hábitats estructuralmente complejos y provee alimentos para muchas especies. Asimismo, la estructura del dosel es considerada una variable esencial de la biodiversidad, pero sólo recientemente puede evaluarse con vehículos aéreos no tripulados (UAV) utilizando nubes de puntos 3D. A pesar de la importancia de los AFS para la conservación, la estructura de su dosel no ha sido evaluada cuantitativamente de manera sistemática, y faltan estudios que traten de analizar la relación entre la estructura del dosel en los AFS y las variables derivadas de las nubes 3D en la región andina.

Aquí muestro cómo pueden predecirse seis importantes variables de la estructura del dosel a través de un gradiente de complejidad desde AFS con cacao y café hasta bosque a partir de las características extraídas de las nubes de puntos 3D utilizando regresiones lineales múltiples. Para el índice de área foliar el mejor modelo obtuvo un R^2 de 0.82 y RMSE relativo = 24%, para la cobertura del dosel un R^2 de 0.81 y RMSE relativo = 13%, para la biomasa aérea R^2 de 0.81 y RMSE relativo = 10%, la densidad de los árboles de sombra fue predicha con un R^2 de 0.66 y RMSE relativo = 34%, la altura media y la desviación estándar de altura en el dosel se predijeron con un R^2 de 0.82 y 0.79 respectivamente, y RMSE relativo del 18% para ambas. El enfoque que se muestra en este estudio puede ayudar a hacer una caracterización precisa de la estructura del dosel usando UAV, lo cual podría ser utilizado para identificar zonas prioritarias de conservación en los paisajes agrícolas.

[*] Trabajo de Grado

[**] Facultad de Ciencias. Escuela de Biología. Maestría en Biología. Director: Björn Reu, Geoecólogo- PhD en Ciencias Naturales.

Abstract

Title: Estimation of forest stand structure in Andean (agro)forests using 3D UAV remote sensing*

Author: Sergio Andrés Bolívar Santamaría**

Key Words: Agroforestry, drone, remote sensing, canopy structure, essential biodiversity variables.

Description: Agroforestry systems (AFS) are of great importance for biodiversity conservation outside protected areas. The composition of crop and shade plants in AFS provides structurally complex habitats and provides food for many species. Also, canopy structure is considered an essential variable of biodiversity, but only recently it can be assessed with unmanned aerial vehicles (UAVs) using 3D point clouds. Despite the importance of AFS for biodiversity conservation, canopy structure has not been quantitatively evaluated in a systematic way, and studies that attempt to analyze the relationship between AFS canopy structure and variables derived from 3D clouds in the Andean region are lacking.

Here, I show how six important variables of canopy structure can be predicted across a complexity gradient from AFS with cocoa and coffee to a natural forest from the characteristics extracted from the 3D point clouds using multiple linear regression. For leaf area index the best model obtained an R^2 of 0.82 with a relative RMSE = 24%, for canopy cover an R^2 of 0.81 and relative RMSE = 13%, for above-ground biomass an R^2 of 0. 81 and relative RMSE = 10%, the density of shade trees was predicted with an R^2 of 0.66 and relative RMSE = 34%, the mean height and the standard deviation of height in the canopy were predicted with an R^2 of 0.82 and 0.79 respectively, and relative RMSE of 18% for both. The approach shown in this study can help make an accurate characterization of the canopy structure using UAVs, which can be used to identify priority conservation areas in agricultural landscapes.

---

* Degree Work

** Faculty of Sciences. School of Biology. Master's in biology. Director: Björn Reu, Geoecologist - PhD in Natural Sciences.

Introduction

Agroforestry systems (AFS) are a land-use type where crops are managed with shade trees and grazing animals (Nair, 1985). In the Andean region AFS are mainly composed of coffee, cacao and a mixture of crops under the shade of trees, which increase the complexity of structure as compared with monocultures. Therefore, AFS have the ability to conserve habitat and provide food for different species and have been recognized as refuges for biodiversity in the tropics (Bhagwat et al., 2008). AFS provide a series of benefits that influence the ecosystem at different spatial scales and dimensions (Jose, 2009); e.g. demonstrating a positive impact on nutrient cycling and the presence of edaphic fauna (Petit-Aldana et al., 2019). In addition, AFS function as corridors for mammals (Williams-Guillén et al., 2006), contributing to improved connectivity at the landscape scale (Asare et al., 2014; Schroth & Harvey, 2007). Specifically, the canopy layer of AFS promotes the regulation of microclimate (Siles et al., 2010; Jiménez-Pérez et al., 2019) and the presence of organisms that facilitate nutrient cycling, pollination and pest control, which can increase productivity at the farm level (Maas et al., 2013). For this reason, it has been suggested that implementing AFS in agricultural land around protected areas can help to conserve biodiversity more effectively (Bhagwat et al., 2008; Swallow et al., 2006). AFS also represents a great opportunity to mitigate the effects of climate change because of their carbon sequestration potential (Nair et al., 2010), as well as social benefits, such as poverty reduction and socio-ecological resilience, because they provide food and multiple economic benefits to farmers (Waldron et al., 2017; Garrity, 2006). The complex structure of AFS and their heterogeneous composition have favored the presence of migratory birds (Díaz-Bohórquez et al., 2014), the abundance of dung

beetles (Neita & Escobar, 2012) and the richness of amphibians in Colombian agroecosystems (Brüning et al., 2018).

In the Colombian Andes, AFS consisted mainly of cacao and coffee crops, under a canopy composed of the genera *Inga* spp., *Erythrina* spp., *Ficus* spp., *Cordia* spp., *Musa* spp. and *Citrus* spp. (Bosselmann et al., 2009; Orozco et al., 2012). These species have shown to have a high carbon fixation capacity (Albrecht & Kandji, 2003; Hernández-Vasquez et al., 2012), allowing to store up to 87.37 Mg ha^{-1} in above-ground biomass (Orozco et al., 2012). Canopy structure of AFS depends largely on the type of management at the farm level (Deheuvels et al., 2012), for example, crop management with low intensity will allow a higher presence of woody plants. In AFS, shade trees represent the largest amount of above-ground biomass and this is related to the volume they occupy (Proulx et al., 2015). For this reason, a valuation of their potential as a carbon sink and their positive effect on habitat conservation can serve to include them into frameworks for payments for environmental services (Bhagwat et al., 2008).

Canopy structure may serve as an indicator of the complexity of the habitat. The characterization of vertical and horizontal vegetation structure has been proposed as an approximation of the heterogeneity and complexity of the habitat (Rutten et al., 2015). Moreover, habitat structure has been defined as one of the Essential Biodiversity Variables (EBV), which are measurements required for study, monitoring and management of biodiversity change (Pereira et al., 2013). The monitoring of habitat structure as an EBV is useful to know the extent of forest or land-use types that provide carbon storage, such as AFS. Ground-based methods such as Terrestrial Laser Scanning (TLS, Seidel et al., 2011), distance-based measurements and hemispheric canopy images have allowed the characterization of tree density (Mitchell, 2010), leaf area index, canopy

cover (Guevara-Escobar et al., 2005) and above-ground biomass (Segura et al., 2006); however, field measurements still require a great deal of time, money and prior knowledge.

The multispectral information captured by satellites allows for estimating biophysical parameters of vegetation such as above-ground biomass (Hall et al., 2006; Kashung et al., 2018), foliar cover (Korhonen et al., 2015; Ma et al., 2017) and the fraction of absorbed photosynthetically active radiation (fAPAR) (Li & Guo, 2016). Satellite information is limited in estimating canopy structure at fines scales because of their coarse resolution (Wulder et al., 2004) and the constant presence of clouds in the tropics.

In order to assess the canopy structure of AFS at a fine scale it is important to achieve a higher spatial and temporal resolution than provided by satellite sensors (Günlü & Kadiogullari, 2018). The development of new remote sensing (RS) technologies, such as unmanned aerial vehicles (UAVs) in recent decades has succeeded in reducing costs for the characterization of canopy structure in a more frequent way (Koh & Wich, 2012; Wich & Koh, 2018). Nowadays, UAVs have become an efficient alternative to perform monitoring of canopy structure at a more detailed level (Paneque-Gálvez et al., 2014). However, there is still no standard method for a simple and rapid assessment and monitoring of AFS and their canopy structure as a biodiversity indicator. Here, I suggest to use the concept of canopy space-filling proposed by Prestzch (2014) to understand the amount of space occupied by tree components (Juchheim et al., 2017). According to Pretzsch (2014), the space-filling can be summarized in two main characteristics, intensity, and scale. The intensity of space-filling refers to the occupation of space in two dimensions, and it is related to the density of trees and foliar cover. On the other hand, the scale of space-filling is related to height distribution of the trees. Greater variability in the canopy height presupposes a greater number of microhabitats for the different species that inhabit the canopy.

Information obtained from the SfM point-clouds has shown to be useful for the three-dimensional characterization (or space-filling) of the canopy at local scales (Wich & Koh, 2018; Iglhaut et al., 2019). Images captured from UAVs with low-cost RGB cameras can be used to generate 3D point-clouds using the Structure from Motion (SfM) photogrammetric range imaging technique (Ullman, 1979). Recently, many open-source or proprietary tools such as Ecosynth, Point Cloud Library (PCL), and Agisoft Metashape, have been developed for the generation, manipulation, and analysis of SfM-derived 3D point-clouds. With these tools the reconstruction of dense point-clouds (between 27 and 117 points per m^2) and estimation of the volume they occupy has become possible (Chang et al., 2018).

Ecological and evolutionary processes in animal assemblages can be affected by the available area and habitat heterogeneity. The species-area relationship (SAR), for example, states that the number of species increases with the surface area (Lomolino, 2000). In terrestrial ecosystems, at regional scales (i.e. islands, landscapes) surface area has been identified as one of the factors which explains biodiversity (Krauss et al., 2004; Steffan-Dewenter, 2003). While at local scale (i.e. farms, plots) heterogeneity in canopy structure has been shown to be an influential factor on microhabitat generation, for beetles (Gatti et al., 2018; Parisi et al., 2019), amphibians and reptiles (Deheuvels et al., 2014; Wanger et al., 2009).

In AFS, high tree density or also high intensity of space-filling has been shown to have a positive impact on the abundance of earthworms and other macroinvertebrates (Pauli et al., 2009; Pauli et al., 2011). While, cover and canopy height have also been associated with increased presence of spiders (Stenchly et al., 2012), birds and bats (Bakermans et al., 2012; Harvey & González Villalobos, 2007). SfM point-clouds accompanied by field sampling have been useful for estimating structural variables that serve as biodiversity indicators (Saarinen et al., 2018).

These include: mean tree height (Jayathunga et al., 2019), basal area, stem volume (Puliti et al., 2015), crown diameter (Panagiotidis et al., 2017) and canopy gaps (Bagaram et al., 2018). In addition, SfM point-clouds data has been used to estimate above-ground biomass and the space-filling for monocultures (Miller et al., 2017) temperate and tropical forests (Kachamba et al., 2016). Characteristics derived from SfM point-clouds have been related to the abundance of frugivorous birds in recovering forests (Zahawi et al., 2015). However, there is a lack of studies looking at AFS and forest that relate variables derived from SfM point-clouds and canopy structure characterized on the ground (Guimarães et al., 2020).

This study aims to estimate AFS canopy structure using variables generated from SfM-point clouds, both related to the space-filling concept. As an application for biodiversity assessments, it will also explore the relationship between space-filling by AFS and the diversity and species composition of birds reported for the study area. I hypothesize that it is possible to predict variables of canopy structure, such as tree height and density of shade trees in AFS using SfM-derived variables.

1. Objectives

1.1. Main objective

To estimate forest canopy structure along a management intensity gradient from low shade agroforests with cacao and coffee to natural forest using drone remote sensing

1.2. Specific objectives

- On ground characterization of forest canopy structure along a management intensity gradient from agroforests with cacao and coffee to near natural forest.
- Quantification of the space-filling of AFS and natural forests using SfM point-clouds obtained with drone images.
- Evaluation of the relationship between (agro)forest canopy structure and space-filling.

2. Methods

2.1. Study area

The study area is a micro-watershed (called *Las Cruces*) which is located in the northern part of the Colombian Andes belonging to the buffer zone of Serranía de los Yariguíes National Natural Park (SYNNP) in Santander. *Las Cruces* encompasses an extension of 5779 ha, has a mean temperature of 22.5 °C; altitudes range between 570 - 2650 m.a.s.l. and annual precipitations between 1500-1700 mm. This area is very important for the water supply and food production of the region, and at landscape level it exhibits an agricultural matrix which is mainly composed by near natural forests, cacao and coffee crops cultivated under shade, as well as monocultures, and some cattle pastures (*Figure 1*.). *Las Cruces* was selected as one of ten study sites of the GEF-Satoyama project across the tropics around the world. *Las Cruces* has been studied between 2016 and 2019; biological, social, and socio-economic assessments were carried out among 12 farms with different levels of agroforest management intensity. Biodiversity assessments were carried out for birds, using a point counts methodology; beetles and ants, using pitfalls and direct captures; and terrestrial vertebrates, studied through camera traps.

Figure 1

Land cover classification of the study area.

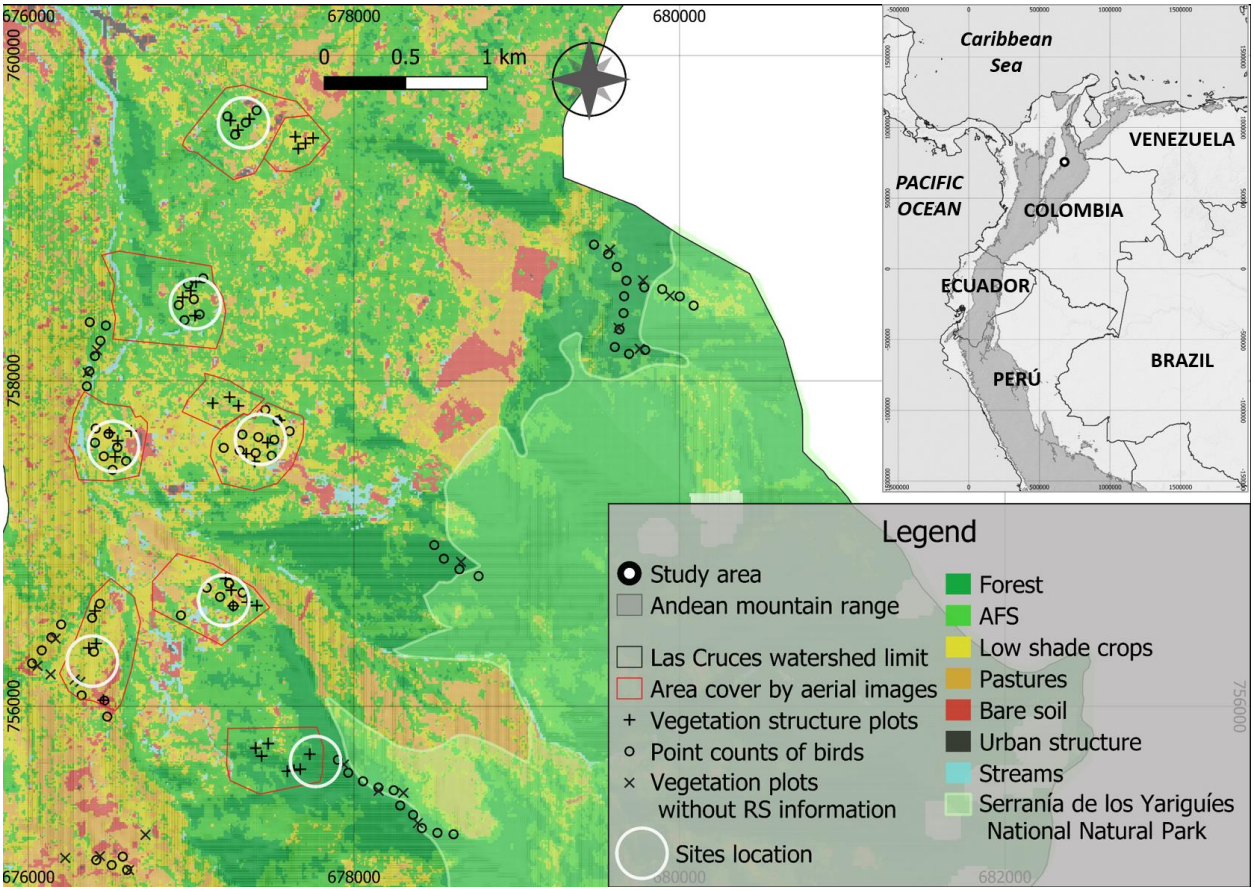

Note. This map is from Bolívar & Reu (under revision) showing the location of field plots and sites. Canopy structure plots are shown as + and x, while bird biodiversity census sites are shown as circles. More detailed orthoimages from each site can be found in the appendix. For the evaluator: Three forest sites lack RS information, which could not be acquired due to the prohibition to visit the study area during the COVID-19 pandemic.

2.2. Sampling design and data acquisition

I carried out the characterization of the canopy structure in 36 plots located in 12 farms along a gradient of management intensity from intact forest (part of SYNNP, 4 plots) to cacao (24 plots) and coffee crops (8 plots) with low shade (*Figure 2.*). I characterized the canopy structure from April to October 2018, taking measurements from crop plants and shade trees using the point centered quarter method (PCQM) (Mitchell, 2010). My plots consist of a rearrangement of point locations in PCQM from a linear transect to a rectangular pattern. This was thought to achieve a high representation of structural heterogeneity inside each plot area and farm. I allocated 9 points every 15m between them inside the crops, getting a 30m x 30m plot (*Figure 3a.*). Using the waypoint averaging function in Garmin Oregon 650, I measured the coordinates of the central point (remeasuring it after 90 min 3 times using waypoint averaging) and corners points (once), in order to achieve the best accuracy of plot position possible. In contrast PCQM in the forest was carried out in two parallel transects with 4 points each and the coordinates of these plots' location were taken based on the average of each of the corner points (*Figure 3b.)*. In each point I divided the space in four quadrants for measuring distances until the nearest neighbor crop plant (in the forest plots this layer is represented by trees lower than 10 m) and the nearest neighbor shade tree, without resampling. In addition, I measured the diameter at breast height ($D_{130} > 2.4$ cm) for shade trees (or D_{20} for coffee and D_{30} for cacao) and measured the height of each sampled plant using a measuring tape or the Forestry Pro II laser rangefinder/hypsometer in the case of shade trees. The measurements using this distance-based method allowed us to estimate tree density, mean height, and mean basal area per plot.

Furthermore, on each AFS plot, I took four images using hemispherical canopy

photography, while three pictures were taken in the forest plots (because the plot design is different in the forest) using a Canon PowerShot G6 with a fish-eye lens (182°, RAYNOX DCR-CF187 PRO). The hemispherical pictures were taken at 1m of height and at twilight, avoiding the direct sunlight to achieve a good contrast between the canopy and the sky. The posterior analysis and estimation of leaf area index (*LAI*) and canopy cover (*CC*) were carried out using Gap Light Analyzer (GLA).

Figure 2

Land-use types considered in this study.

Note. a) Near intact forest, b) agroforestry system with cacao, c) agroforestry systems with coffee.

Figure 3

Plot design for on-ground characterization of canopy structure in AFS.

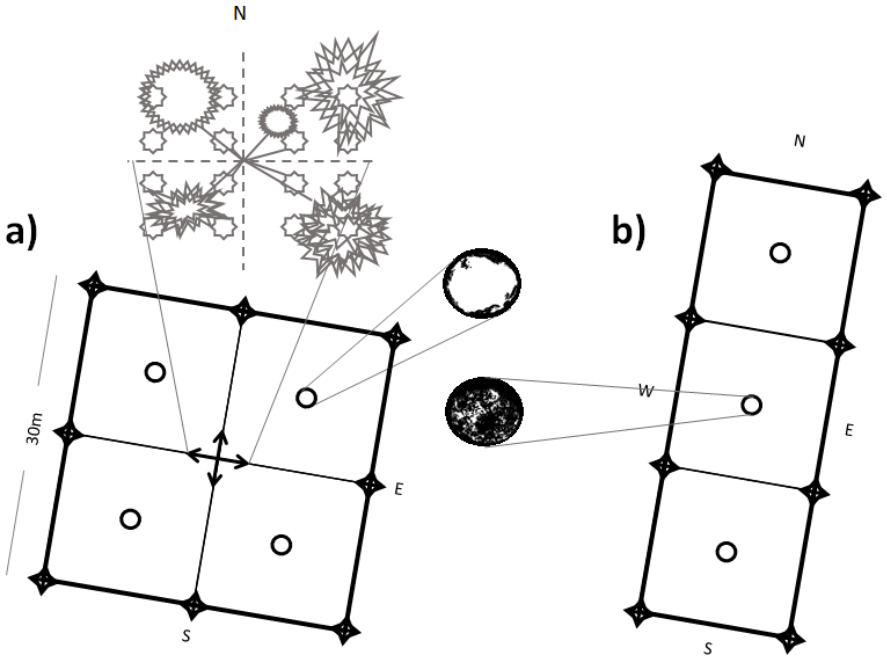

Note. (a) and forests (b). Each sampling location for the Point-Centered-Quarter Method (PCQM) is shown with an arrow cross. Circles show the positions for hemispherical photography acquisition.

2.2.1. On-ground variables estimation

I estimated the density of crop and shade trees (number of individuals per plot area, *D_mid* & *D_over*, respectively) based on the average distance from the nearest neighbor using PCQM. I then added correction factors for estimated densities on each canopy layer; these were determined by the number of quadrants without sample (Mitchell, 2010; Warde & Petranka, 1981). Using the diameter (D_{20} , D_{30}, D_{130}) I calculated the basal area (BA) of each plant as $radius^2*\pi$, then I

calculated the sum of BA and the mean height per plot. I used Gap Light Analyzer (GLA) software to estimate the *LAI* and *CC* for each of the hemispheric pictures taken on the plots, after this, I calculated the plot average. In addition, using allometric equations, I estimated above-ground biomass (*AGB*) for coffee (Segura et al., 2006), cacao, citrus fruits, and Musaceae plants (Somarriba et al., 2013) as well as shade trees (Alvarez et al., 2012). Due to the lack of species information in forest plots, for their allometric equations I used the average of wood density registered in a permanent forest plot from Alvarez et al. (2012) in San Vicente de Chucurí, which is close to the study area. With this I estimated the average of *AGB* for crop plants and shade trees and multiplied it by the number of individuals in each layer, the sum of these values was considered the total *AGB* estimated with the ground sampling data (Table 1.). We used Principal Component Analysis (PCA) to assess the main gradient in canopy structure across the plots of different land-use types.

Table 1

Canopy structure variables estimated from on-ground measurements.

Variable	Abbreviation	Units	Mean	Range
Leaf area index	*LAI*	unitless	1.64	0.07 - 3.28
Canopy cover	*CC*	%	69.03	19.45 - 92.08
Above ground biomass	*AGB*	Mg ha^{-1}	78.81	4.38 - 391.1
Density of overstory trees	*D_over*	# of shade trees/ plot	15.14	0.68 - 69.15
Mean heigt of shade trees	*H_over*	m	11.52	2.84 - 24.50
Standard deviation of shade trees' height	*H_sd_over*	m	4.83	1.36 - 9.51
Density of midstory plants	*D_mid*	# of crop plants/ plot	189.46	46.21 - 703.45
Mean heigt of crop plants	*H_mid*	m	3.24	1.13 - 6.30
Standard deviation of crop plants' height	*H_sd_mid*	m	0.84	0.30 - 2.52

*N*ote. In forest plots D_mid denotes the number of trees per plot with a height < 10m, while D_over denotes the number of trees over 10m.

2.3. Remote sensing data and processing

2.3.1. Capture of UAV photographs

The aerial images were collected with a fixed wing drone “UAV Mapper” produced by TuffWing LLC, which has a flight autonomy of 45 minutes and the capacity to cover an area of approximately 100 Ha. The UAV Mapper also has an Inertial Measurement Unit (IMU) that allows

a basic stabilization during the flight to achieve zenital images. The UAV Mapper was equipped with a Canon S110 camera to acquire high resolution (.raw) RGB images, using a modified intervalometer script (Canon Hack Development Kit, CHDK). The Canon S110 has 12.1 MP of resolution, the focal length used to take pictures was 24 mm, while the aperture and ISO have automatic adjustment.

Nine autonomous flights were designed in Mission Planner software (v1.3.11) (Oborne, retrieved from http://planner.ardupilot.com/) and carried out considering the geography of each site and an overlap over 90% between images in agreement with Frey et al. (2018). This allowed to cover all farms and forest area where canopy structure has been measured. An informed consent was signed by each farm owner giving permission to take the aerial photographs. Using a PC and the telemetry antenna as ground station, a team composed of observer and pilot (previously certificated by APD, official page: https://apd.ong/) executed and monitored the flight plans with Mission Planner (MP). The photographs were taken on a clear day, early in the morning or around noon to minimize the effects of wind and shadows. In order to improve the accuracy of the location of 3D point-clouds we took coordinates with waypoint average function to use them as Ground Control Points (GCPs) along the photographed area. We geotagged each photograph with correct coordinates using the Geo tagging tool in Mission Planner.

2.3.2. 3D point cloud generation

Because of the high demand of data processing, all analyses were conducted in a Dell Precision tower 5810 Intel® Xeon® Processor E5-1620 v3 with a NVIDIA® Quadro®. I used Agisoft Metashape Professional (v1.6.2) (Agisoft LLC, St. Petersburg, Russia, 2019) for the

reconstruction of orthomosaics (union of many photographs that are geometrically corrected) and SfM point-clouds (set of points in space, which have coordinates in the three axes, x, y and z) with the aerial images. In Agisoft, I defined high accuracy in the alignment of the photographs and thereafter I built the SfM point-clouds with a high level of quality. Based on SfM point-clouds I reconstructed the Digital Surface Model (DSM, raster which includes all objects over the earth's surface). Finally, I exported SfM point-clouds in .las format and rasters with a Ground Sampling Distance (GSD) of 7 cm/pixel (i.e. orthomosaics and DSM) as .tiff files for further analysis.

2.4. Data analyses

2.4.1. Feature extraction from 3D point clouds

In summary, I generated 54 variables as proxies of the space-filling for 62 plots characterized on ground. However, 26 plots were not included in the analysis (presented with x in Figure 1.), if plantations were renewed (16 plots) or if aerial images in forest (over 10 plots) could not be obtained because of technical limitations. In order to predict the canopy structure variables obtained with on ground information (i.e. LAI, CC, AGB, height or density of trees) using 3D variables extracted from SfM point-cloud of each plot (related to space-filling concept). I handled and processed all the information exported by Agisoft using the R packages "raster", "lidR", "rgdal", "glcm", "geometry". First, I used the "lidR" package in R to crop the .las files using a 20 m radius circumference around the centroid of each plot (*Figure 4.*). I manually removed the outliers points in Agisoft Metashape Professional. Then, I classified the lowest points on each plot using a progressive morphological filter (pmf function of "lidR" package) and made a spatial

interpolation using delaunay triangulation algorithm to obtain the Digital Terrain Model (DTM, bare ground surface without vegetation). Afterwards, I subtracted each DTM to their specific 3D point cloud using the lasnormalize() function and then, I deleted points below 0 meters, in order to obtain a clean Canopy Height Model (CHM, Height of vegetation on each pixel, *Figure 5*.). Using the CHM of each plot with an aggregated GSD of 30 cm/pixel, I calculated the mean, standard deviation, the skewness, maximum value and entropy of heights, I calculated the Vertical Complexity Index (*VCI*, sd of height/mean of height), Vertical Distribution Ratio (*VDR*, maximum height -median of height/maximum height), the percentiles of heights every 10% (*Q10, Q20… Q90*), density of heights over quartiles (*denq25, denq50, denq75, denq90*), CHM surface area using convex hull of point clouds (*area_chull*), volume based on voxels (*v_voxels*, Frey et al., 2018) as 3D predictors. Textural features as homogeneity, contrast and dissimilarity, proposed by Haralick et al. (1973) were also estimated based on CHM (i.e. height raster) using the "glcm" package in R. Finally, I calculated the proportion of area cover by pixels over each height every 2 m (i.e. s2 = relative area cover by pixels over 2 m, s4, s6, s8… s32) and, I extracted the values of probability distribution of heights between 0-1.25 m, 1.25-4.5m and higher than 4.5 m (Table 2.).

Figure 4

RGB zenithal view of point clouds from each of 36 plots used in this study.

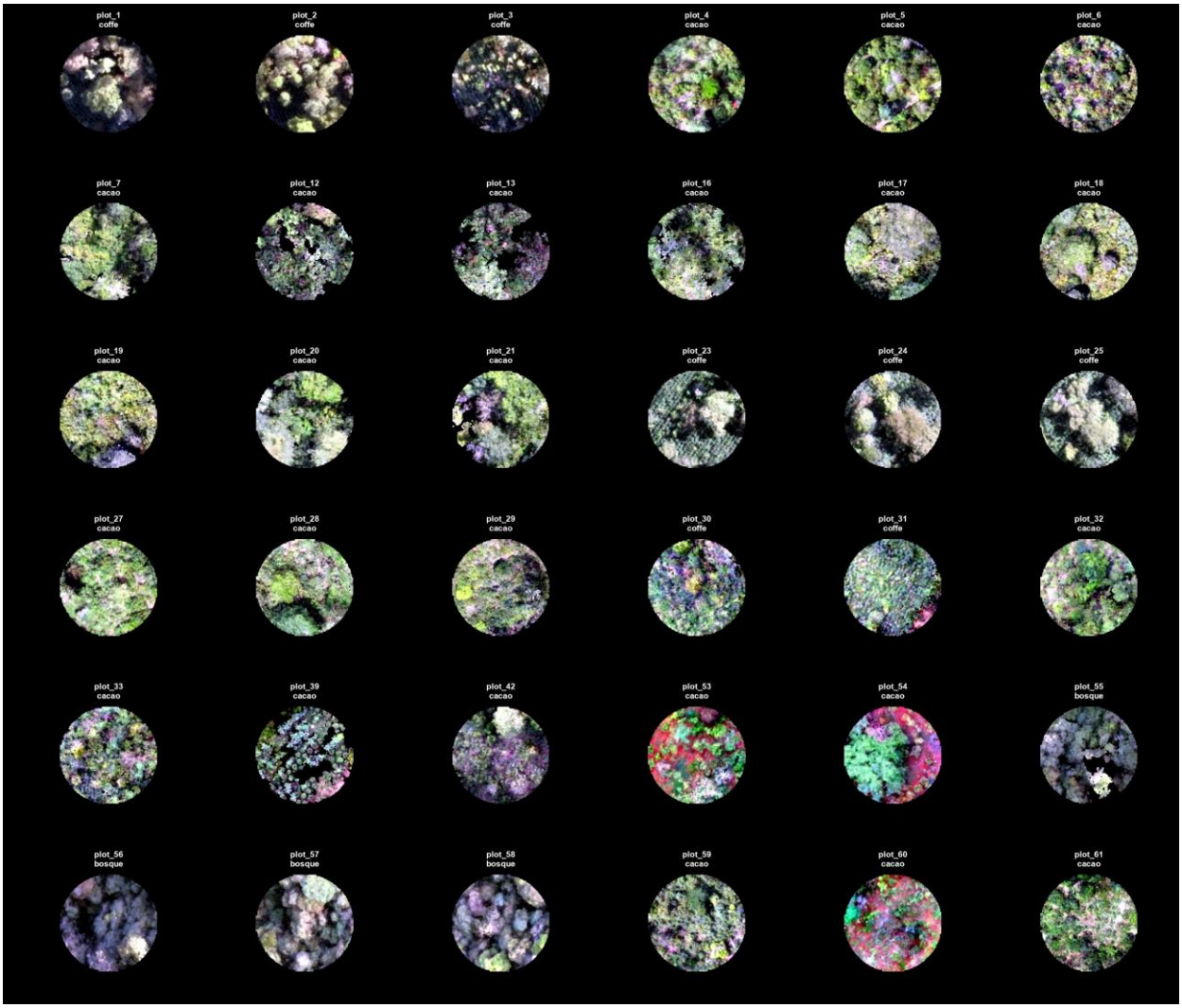

Note. The radius of each circle is 20 meters.

Figure 5

Canopy height models (CHM) of 36 plots used in this study.

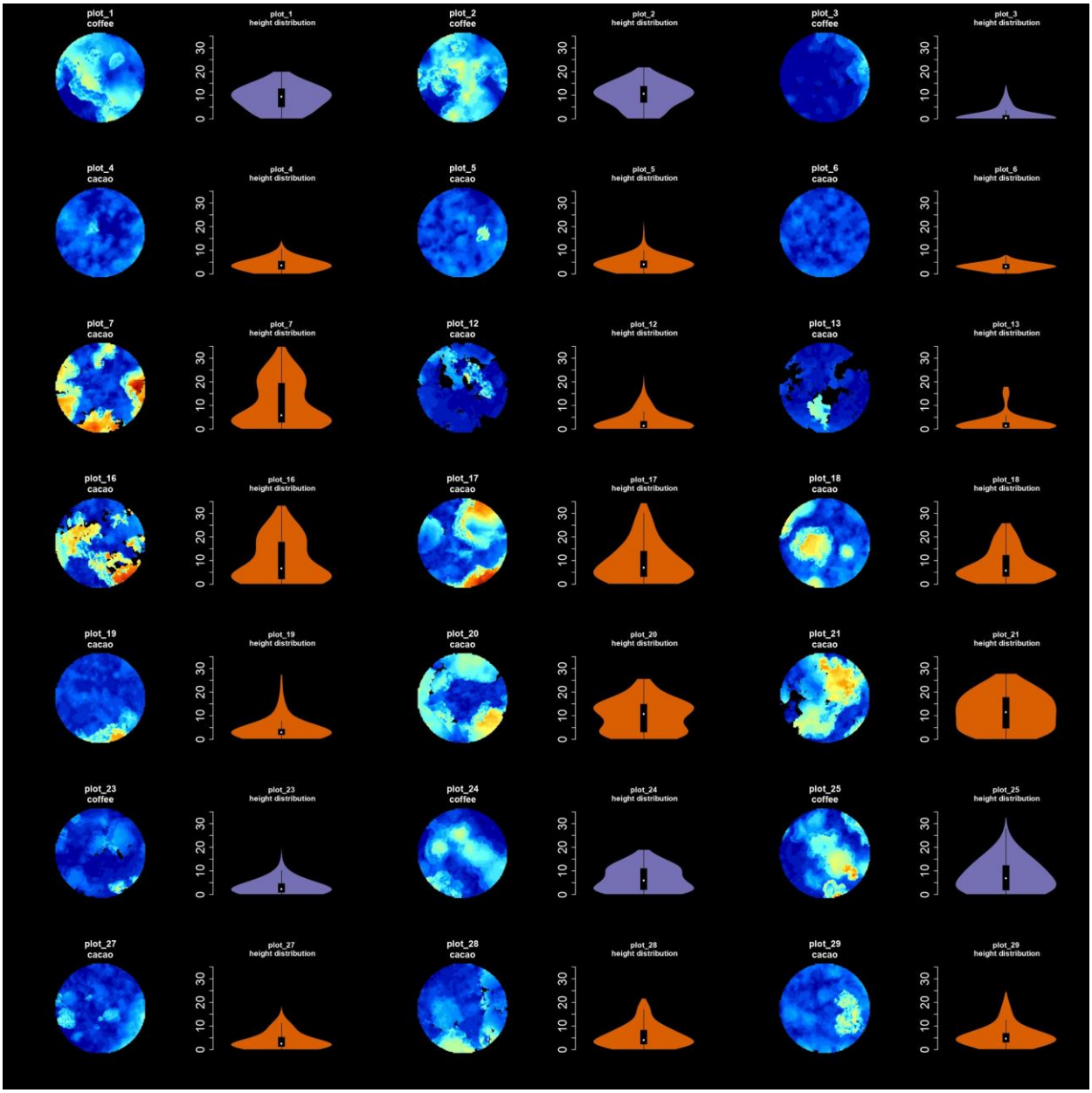

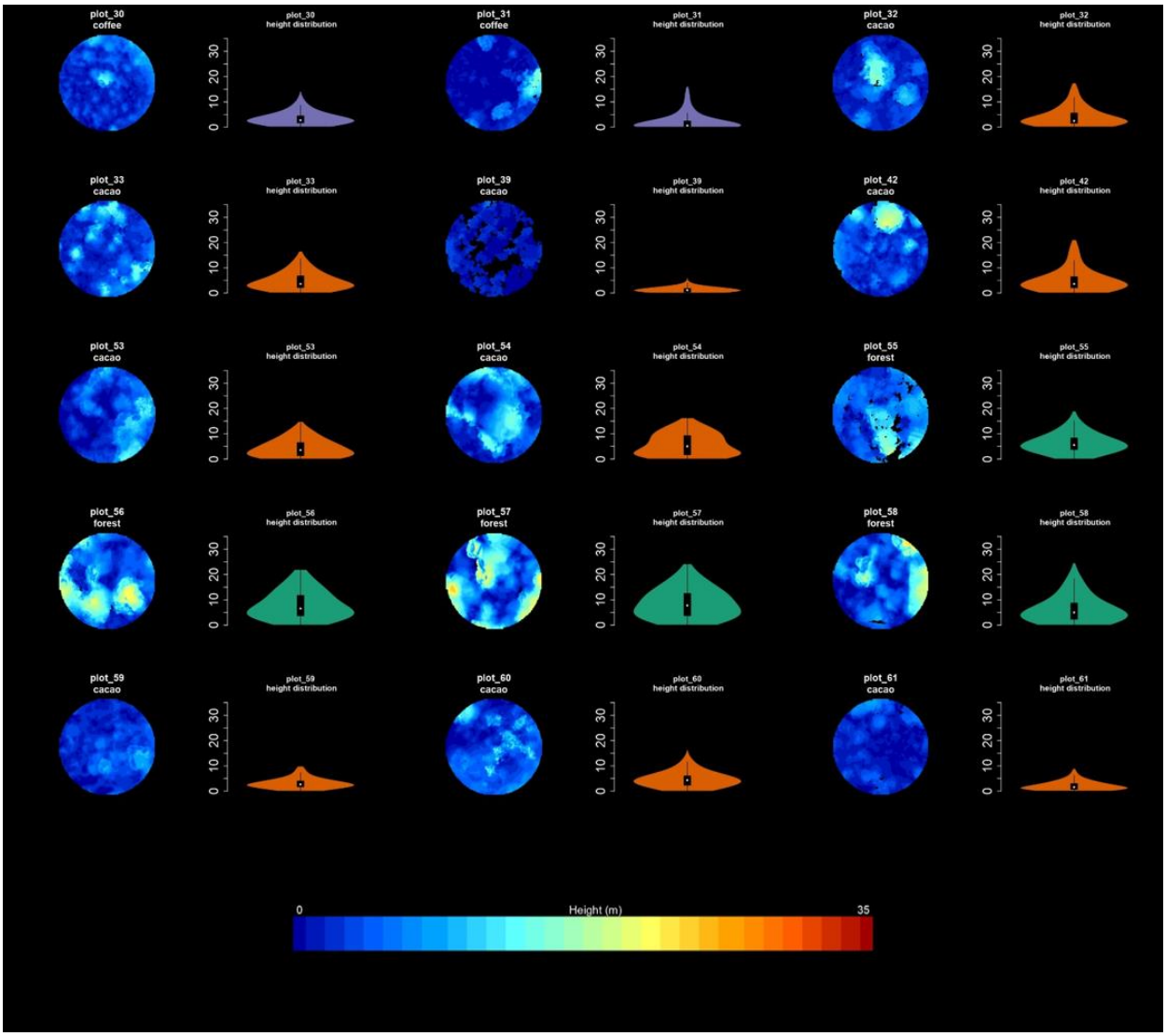

Note. The height distribution of grid-cells of each CHM is shown as a violin. The color of the violins represents land-use type: purple for AFS with coffee, orange for AFS with cacao and green for forest plots. Black areas have no information.

Table 2

3D variables derived from canopy height models of 36 plots used in this study.

Variable name	Units	Description
hmean	m	Mean of Canopy Height Model (CHM)
hsd	m	Standard deviation of values in CHM
hskew	unitless	Skewness of the distribution in CHM values
hmax	m	Maximum value in CHM
hentropy	unitless	Normalized Shannon diversity index of CHM values
hmedian	m	Median of values in CHM
COVAR	unitless	Coefficient of variation of heights = sd of heights/mean of heights on each point cloud
VCIm	–	Vertical Complexity Index, based on .las cloud. van Ewijk et al. (2011).
VCIsd		Standard deviation of VCI
VDR	between 0 - 1	Vertical Distribution Ratio, VDR = max-median/max. (Goetz et al., 2007)
denq25, denq50, denq75, denq90	m/pixels	Density of height over each quantile (sum of heights over each quantile/total number of pixels)
area_chull	m^2	Area cover by the convex hull of each point cloud
v_voxels	m^3	Volume estimated through voxel aproximation
glcm statistics (mean, variance, homogeneity, contrast, dissimilarity, entropy, second momento)	–	Textural features computed from a Gray Level Co-ocurrence Matrix (Haralick et al., 1973). CHM were the imput matrix and 3x3 window was used in analysis
Q1, Q20, Q30… Q90	m	Quantiles of heights in each CHM
s2, s4, s6, s8, s10… s32	unitless	Relationship between area cover by pixels over each height and total area cover by plot
s1.25_mean, s1.25_med, s1.25_max	between 0 - 1	Relative likelihood of heights between 0 -1.25 meters
s4.5_mean, s4.5_med, s4.5_max		1.25 - 4.5 meters
s10_mean, s10_med, s10_max		and 4.5 - 10 meters

2.4.2. Canopy structure vs 3D variables

I used linear models (eq. 1) to predict *LAI*, *CC*, *AGB*, *D_over*, *H_over* and *H_sd_over* from 3D variables. To do so, I (1) calculated the Variance Inflation Factor (VIF) to exclude the highly correlated 3D variables, then (2) using the selected variables and the category of land-use type I constructed multiple linear regression models for each dependent variable, and (3) I ran a stepwise

selection of the variables to select the best model based on the Akaike Information Criterion (AIC). Finally, I removed from models, predictor the variables that were not statistically significant for them. To test the accuracy and calculate the variables coefficients of final models, I ran a 10 k-fold cross validation with 10 iterations using the "caret" package (Kuhn, 2008). Based on cross validation I calculated the coefficient of determination (R^2), Mean Absolute Error (MAE, eq. 2), Root Mean Square Error (RMSE, eq. 3), AIC and Relative Root Mean Square Error (RRMSE, eq. 4) of models' prediction with its additive and interactive term using as dummy predictor the land-use type. Finally, I ran a prediction using the best models and made a regression between predicted and observed values. To facilitate interpretation and for comparison purposes I considered an R^2 lower than 0.5 a low correlation, between 0.5 - 0.7 as a good correlation and above 0.7 a strong correlation, as proposed by Guimarães et al. (2020)

$$Y = \beta_0 + \beta_1 X_1 + \beta_2 X_2 + \ldots + \beta_p X_p + \varepsilon \quad \text{(eq. 1)}$$

$$MAE = \frac{1}{n}\sum_{j=1}^{n}\left|y_j - \widehat{y_j}\right| \quad \text{(eq. 2)}$$

$$RMSE = \sqrt{\frac{1}{n}\sum_{j=1}^{n}(y_j - \widehat{y_j})^2} \quad \text{(eq. 3)}$$

$$RRMSE = \frac{\sqrt{\frac{1}{n}\sum_{j=1}^{n}(y_j - \widehat{y_j})^2}}{\frac{1}{n}\sum_{j=1}^{n} y_j} x100 \quad \text{(eq. 4)}$$

2.4.3. Canopy structure vs diversity and species composition of the avifauna

In order to demonstrate the importance of canopy structure on AFS habitat structure I used a data set on bird diversity and species composition obtained in a previous study (Fromm, 2019). To do so, I added canopy structure and 3D variables from plot-level to site-level (i.e. farm or cultivation level) according to the sampling design used by Fromm (2019). I used the abundance of birds, biodiversity indices such as species richness and the Shannon index as well as species composition to demonstrate the relationship of these variables with canopy structure. Species composition was summarized in the first two axis of a Principal Coordinate Analysis (*pcoa1* and *pcoa2*) using a species abundance matrix at the site level and the Bray-Curtis dissimilarity. Finally, I used Principal Component Analysis (PCA) to explore the relationship among variables. I noted that this analysis is a simple demonstration about a potential application of the work on canopy structure presented here (and not the objective). I also evaluated the accuracy of predictive models for canopy variables at site-level using a 3 k-fold cross validation with 100 replicates.

3. Results

3.1. Gradient in canopy structure

The multivariate analysis of canopy structure using PCA revealed a canopy structure gradient across the plots located in AFS (i.e. first PCA axis) and between AFS and forest plots (i.e. second PCA axis). The first axis explains 50.3 % of variance and is mainly related to height in midstory (*H_mid*), leaf area index (*LAI), c*anopy cover (*CC*) and above-ground biomass (*AGB*). The second axis represents the 18.2% of the variance and the most related variables are density of shade trees (*D_over),* sum of basal area of midstory plants (*BA_mid*), standard deviation of height in overstory trees (*H_sd_over*) and density of midstory plants (*D_mid*, see *Figure 6.*). Therefore, apart from crops' height (*H_mid*), differences between AFS with coffee and cacao are due to the amount of *AGB* and LAI. Otherwise, the density of shade trees (*D_over*) are similar for both types of AFS analyzed. The PCA also reveals a higher variation of height in the overstory (*H_sd_over*) for forests and AFS with cacao, while on AFS with coffee there is a lower percentage of canopy cover (*CC*) and higher density of crop's plants (*D_mid*) than the cacao plots.

Figure 6

Ordination plot with on-ground variables.

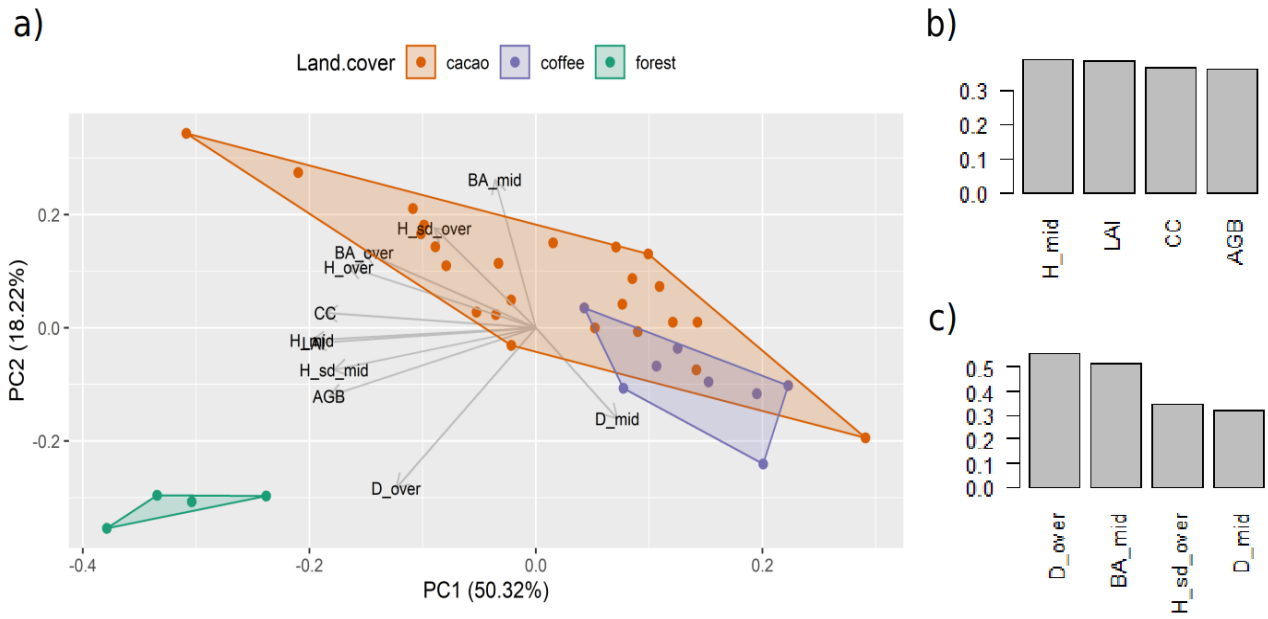

Note. a) Ordination of plots according to their canopy vegetation structure derived from Principal Component Analysis b) shows variables with high loading on PC1 and c) shows Variables with high loading on PC2. H stands for height; BA for basal area; D, is density of individuals in the midstory (mid) or overstory (over); CC, is canopy cover and AGB, is for above-ground biomass.

The analysis of the canopy height models (CHMs) reveal systematic differences in height distribution among land-use types (*Figure 7.*), despite the fact that there is a great variation in height distribution among plots (*Figure 5.*). AFS with coffee show the highest values of probability distribution below 1.25 meters height, while AFS with cacao show the highest probability distribution between 1.25 and 4.5 meters height. The forest shows a broader range of probability of heights, mainly between 1.5 and 10 meters height, also with higher density in the upper canopy (from 12.5 meters onwards) as compared to the AFS. Based on those differences, I decided to

include the mean, median, standard deviation and maximum values of probability distribution of heights (i.e. height distribution between these ranges, 0-1.25 m; 1.25-4.5m and 4.5-10 m) as predictor variables in the models, because of their potential to distinguish between land-use types.

Figure 7

Probability distribution of heights derived from the Canopy height models of the three land-use types.

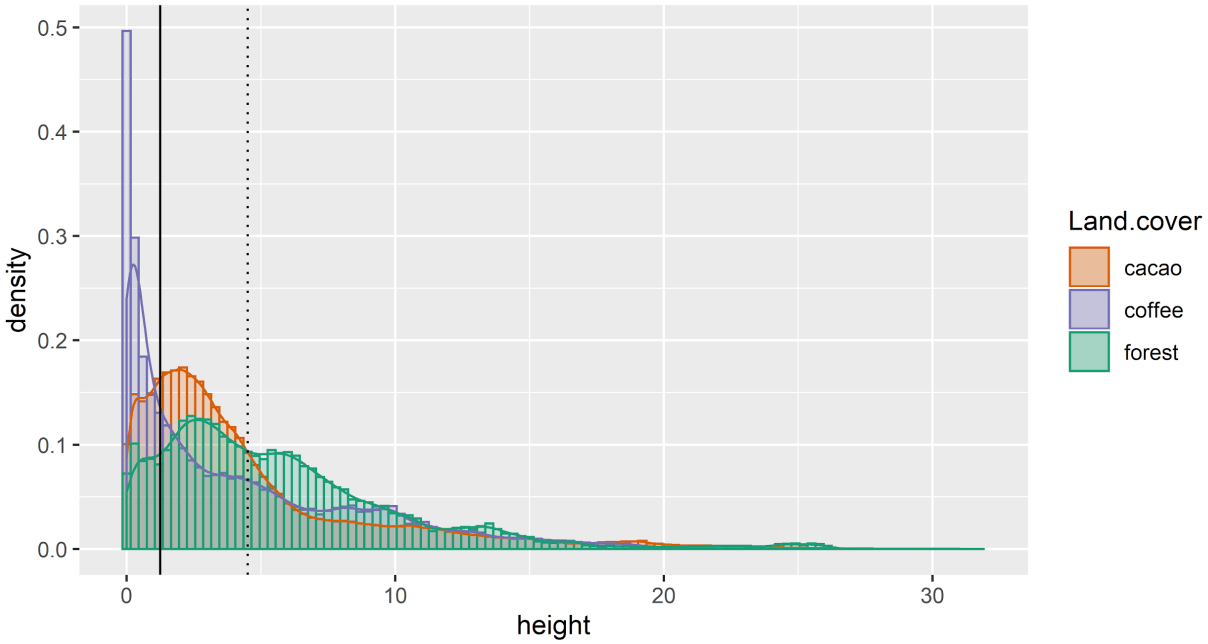

Note. The solid line marks 1.25 m height and the dotted line 4.5 m height, which are important thresholds showing in 3D predictors.

A PCA using the 54 3D variables derived from SfM point-clouds listed in Table 1. didn't show a clear separation of the three land-use types (*Figure 8a.*), indicating that not all predictor variables might be useful for considering them to distinguish canopy structure. For example, the

majority of 3D variables in the forest plots are not different from those found in AFS plots, there is also a greater variability of 3D variables in AFS with coffee than those found in forest. On the other hand, an ordination of plots using just variables extracted from probability distribution of heights showed a better distinction between forest and AFS plots (*Figure 8b.*).

Figure 8

Ordination plot with 3D variables.

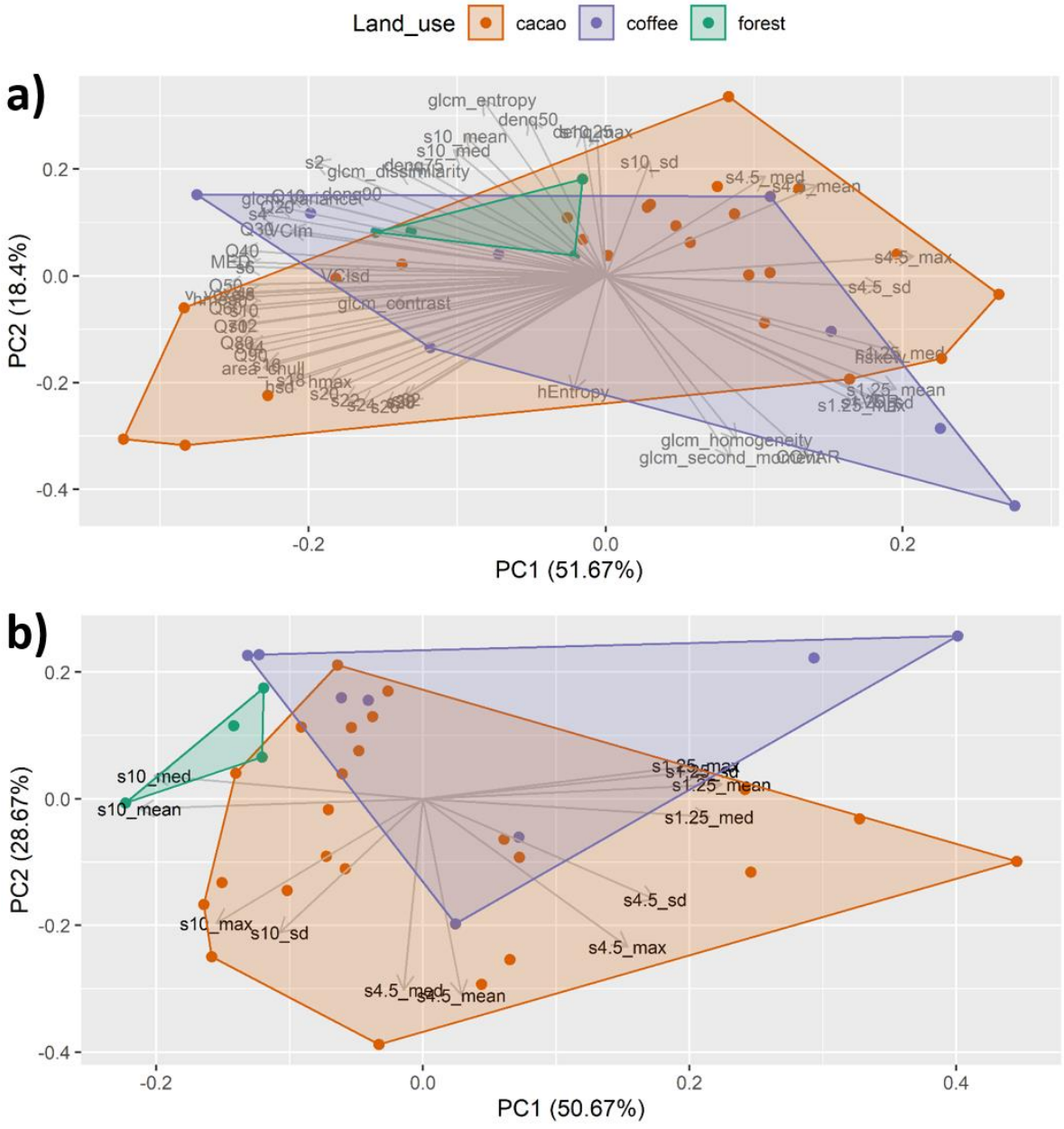

Note. a) PCA based on all 3D variables generated from canopy height models. b) PCA based only on variables derived from the probability distribution of heights. All variables used for this analysis are listed and described in Table 1.

3.2. Predicting canopy structure from 3D variables

3.2.1 Relationship between canopy structure and 3D variables at the plot-level

During model construction 3D variables showed strong correlations among them and resulted in an elimination of the majority based on VIF and subsequent stepwise variable selection. For LAI the best model indicated by AIC includes the variables *hskew, hEntropy, VCIsd, denq75, s1.25_max, s4.5_sd* and *Land-use* and resulted in predictions with an R^2 of 0.82 after 10-fold cross-validation. For *CC* the best model resulted in predictions with an R^2 of 0.81 (also after 10-fold cross-validation) and a relative root mean squared error (RRMSE) of 13%; this model includes *hskew, VCIsd, denq75, COVAR, Q10, s4.5_sd* and *Land-use.* The best model for *AGB* showed the lowest RRMSE (10%) among all models with a $R^2 = 0.81$. This was the only model which included textural features such as *glcm_contrast* and *glcm_second_moment,* as well as *denq75, s4.5_sd* and *s4.5_med,* indicating that for AGB the height distribution of the CHM is less important. For density of overstory trees (*D_over*) the best model includes *hEntropy, denq90, area_chull, s32, s1.25_max, s4.5_sd, s10_sd* and *Land_use,* achieving a good prediction with a $R^2 = 0.66$. The predictive model for the height of overstory trees (*H_over)* includes only three variables *area_chull, s4.5_sd* and *Land-use,* achieving a $R^2 = 0.82$ and RRMSE = 18%. Finally, for the variation of height distribution in the overstory layer (*H_sd_over)* the best predictive model includes *hmax, VCIsd, COVAR, Q10* and *Land-use* and resulted in predictions with an $R^2 = 0.79$.

Table 3

Regression model accuracy metrics for multiple linear models fitted to each dependent variable.

Model	R^2	RMSE	MAE	AIC	RRMSE
LAI ~ hskew + hEntropy + VCIsd + denq75 + s1.25_max + s4.5_sd	0.7	0.66	0.56	75.44	40%
LAI ~ hskew + hEntropy + VCIsd + denq75 + s1.25_max + s4.5_sd + Land-use	0.82	0.39	0.33	38.94	24%
LAI ~ hskew + hEntropy + VCIsd + denq75 + s1.25_max + s4.5_sd * Land-use	0.76	0.58	0.44	42.87	35%
CC ~ hskew + VCIsd + denq75 + COVAR + Q10 + s4.5_sd	0.63	12.34	10.8	285.46	18%
CC ~ hskew + VCIsd + denq75 + COVAR + Q10 + s4.5_sd + Land-use	0.81	8.8	7.72	260.99	13%
CC ~ hskew + VCIsd + denq75 + COVAR + Q10 + s4.5_sd * Land-use	0.73	11.58	9.67	264.81	17%
log(AGB) ~ denq75 + glcm_contrast + glcm_second_moment + s4.5_med + s4.5_sd	0.58	0.68	0.57	82.02	17%
log(AGB) ~ denq75 + glcm_contrast + glcm_second_moment + s4.5_med + s4.5_sd + Land-use	0.81	0.41	0.36	41.56	10%
log(AGB) ~ denq75 + glcm_contrast + glcm_second_moment + s4.5_med + s4.5_sd * Land-use	0.77	0.55	0.44	38.23	14%
D_over ~ hEntropy + denq90 + area_chull + s32 + s1.25_max + s4.5_sd + s10_sd	0.45	17.23	13.59	316.08	114%
D_over ~ hEntropy + denq90 + area_chull + s32 + s1.25_max + s4.5_sd + s10_sd + Land-use	0.66	5.15	4.53	216.55	34%
D_over ~ hEntropy + denq90 + area_chull + s32 + s1.25_max + s4.5_sd + s10_sd * Land-use	0.65	5.11	4.47	215.42	34%
H_over ~ area_chull + s4.5_sd	0.8	2.28	1.89	168.25	20%
H_over ~ area_chull + s4.5_sd + Land-use	0.82	2.06	1.72	160.46	18%
H_over ~ area_chull + s4.5_sd * Land-use	0.78	3.19	2.37	163.38	28%
H_sd_over ~ hmax + VCIsd + COVAR + Q10	0.78	0.96	0.8	105.41	20%
H_sd_over ~ hmax + VCIsd + COVAR + Q10 + Land-use	0.79	0.89	0.74	100.68	18%
H_sd_over ~ hmax + VCIsd + COVAR + Q10 * Land-use	0.75	1.33	0.99	103.02	27%

Note. all values are based on a repeated 10 k-fold cross validation.

In general, taking land-use type into account as a predictor variable significantly reduced the AIC in the models (Table 3.). The additive form of the models showed the lowest AIC, but the interactive form of models for *AGB* and *D_over* obtained similar AIC values as the additive ones. Besides land-use type, the most used quantitative variable in predictive models, was the standard deviation of probability distribution between 1.25 and 4.5 m (*s4.5_sd*), followed by density of heights over 75% percentile (*denq75)* and the standard deviation of vertical complexity index (*VCIsd*, more details in Table 5.*)* all of which are derived from the vertical height distribution of the CHMs. Since almost all models improved when land-use type (i.e. AFS with cacao, AFS with coffee or forest) variable was included as predictor, the evidence indicates that a certain amount of structural variation among land-use types remains uncaptured by 3D variables derived from SfM point-clouds.

The evaluation of the calibration of the models, using simple linear regression between

predicted vs observed (PO) response values (*Figure 9*.) reveals that the slope is not significantly different from 1 and the bias is constant across the ranges. The PO charts for *LAI*, *CC*, *AGB* and *D_over*, showed marked differences (i.e. higher values) of observed values between forest and AFS, while for *H_over* and *H_sd_over* these values did not differ. Also, for the predicted values of height variables (mean, sd) AFS plots had similar or even higher values than those found in forest.

Figure 9

Predicted vs observed scatter plots, using the best linear model for each variable.

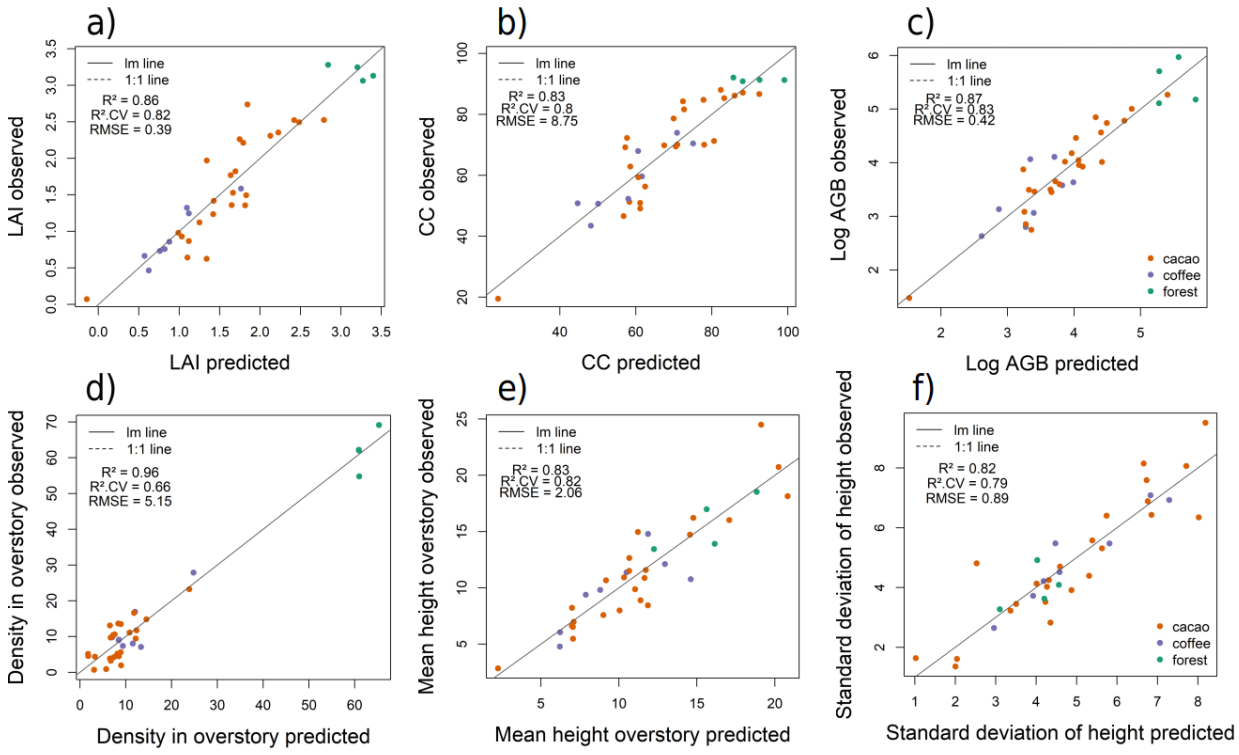

Note. a) Leaf area index (*LAI*), b) Canopy cover (*CC*), c) Logarithm of above-ground biomass (*log AGB*), d) Density of overstory trees (*D_over*), e) Mean height of overstory trees (*H_over*), f) Standard deviation of height in overstory layer (*H_sd_over*). R².CV is for cross-validated R².

Table 4

Regression model accuracy metrics for multiple linear models fitted to each predictor variable at the site-level.

Model	R^2	RMSE	MAE	AIC	RRMSE
LAI ~ denq90	0.86	0.9	0.83	18.76	52%
LAI ~ denq90 + area_chull	0.82	0.93	0.85	16.88	54%
LAI ~ denq90 + area_chull + glcm_mean	0.91	0.63	0.59	3.76	37%
CC ~ denq90	0.83	16.15	14.72	60.11	23%
CC ~ s1.25_max	0.89	14.43	13.27	56.65	20%
CC ~ denq90 + s1.25_max	0.87	19.58	18.1	53.63	28%
log(AGB) ~ denq90	0.88	0.75	0.65	17.53	18%
log(AGB) ~ denq90 + area_chull	0.84	0.79	0.7	14.77	19%
log(AGB) ~ denq90 + area_chull + glcm_second_moment	0.86	1.27	1.18	10.92	30%
D_over ~ denq90	0.9	22.07	18.1	61.35	130%
D_over ~ denq90 + denq75 + VCIsd	0.85	22.64	18.49	50.63	134%
D_over ~ denq90 + denq75 + VCIsd + hEntropy	0.85	17.36	14.38	28.18	102%
H_over ~ Q10	0.87	3.93	3.48	41.43	31%
H_over ~ Q10 + s30	0.87	3.72	3.4	37.05	30%
H_over ~ Q10 + s30 + s4.5_med	0.88	3.02	2.5	20.94	24%
H_sd_over ~ hmax	0.9	1.35	1.26	25.31	25%
H_sd_over ~ hmax + glcm_mean	0.86	2.07	1.85	26.18	38%
H_sd_over ~ hmax + glcm_mean + COVAR	0.93	1.78	1.6	4.18	33%

Note. All statistics are based on a 100 repeated 3-fold cross-validation

3.2.2. Relationship between canopy structure and 3D variables at site-level

Based on the AIC, the best model for LAI prediction at site-level used *denq90*, *area_chull* and *glcm_mean* and showed an R^2 = 0.91 (RRMSE = 37%). For prediction of *CC*, were used *denq90* and *s1.25_max* in the best model, this model yielded an R^2 = 0.81 and 28% of relative RMSE. The best model to predict *AGB* was composed by *denq90*, *area_chull* and *glcm_second_moment* as predictors, achieving a R^2 = 0.86 and a 30% of RRMSE. The best model for *H_sd_over* had the highest R^2 = 0.93 among all models, and a RRMSE of 33% using *hmax*, *glcm_mean* and *COVAR* as predictors (Table 4.).

Table 5

The most important predictors and the number of its appearances on the best models at plot-level.

Predictor variable	# of model appearances	*LAI*	*CC*	*log(AGB)*	*D_over*	*H_over*	*H_sd_over*
Land.cover	6	x	x	x	x	x	x
s4.5_sd	5	x	x	x	x	x	
denq75	3	x	x	x			
VCIsd	3	x	x				x
hskew	2	x	x				
hEntropy	2	x			x		
s1.25_max	2	x			x		
COVAR	2		x				x
Q10	2		x		x		
area_chull	2				x	x	
hmax	1						x
denq90	1				x		
s4.5_med	1			x			
s10_sd	1				x		
glcm_contrast	1			x			
glcm_second_moment	1			x			
s32	1				x		

The most useful variable for predictive models at site-level was density of heights over the 90% quantile (*denq90*). In fact, the models which only include *denq90* show high accuracy to predict *CC* and *AGB* with 77% and 82%, respectively. The inclusion of *area_chull* in the *LAI* and *AGB* models decreases the R^2 and the accuracy (i.e. higher RRMSE), but also reduces the AIC. Textural features as *glcm_mean* and *glcm_secon_moment* improve predictions of *LAI* and *AGB* at site-level. Finally, the maximum value in CHMs (*hmax)* was only important for prediction of *H_sd_over*.

Table 6

The most important predictors and its number of appearances on the best models at site level.

Predictor variable	# of model appearances	*LAI*	*CC*	*log(AGB)*	*D_over*	*H_over*	*H_sd_over*
denq90	4	x	x	x	x		
area_chull	3	x		x			
s1.25_max	1		x				
COVAR	1						x
Q10	1					x	
hmax	1						x
s4.5_med	1					x	
glcm_mean	1	x					x
s30	1					x	
VCIsd	1				x		
hEntropy	1				x		
denq75	1				x		
glcm_second_moment	1			x			

3.3. The importance of canopy structure for the diversity and composition of the avifauna

Using canopy structure variables as predictors for the diversity and species composition of the avifauna present in the study area reveals interesting relationships. There are stronger relationships between canopy structure variables, bird abundance and composition, than canopy structure and bird biodiversity. All relationships are negative, *CC*, *LAI* and *AGB* explained between 37% and 44% of bird biodiversity (*Figure 10.*, upper row), while they explained between 47 and 70% of the variation in bird abundance (*Figure 10.*, middle row). For 3D variables the most related variable to richness, Shannon's diversity index and abundance of birds was *s10_max* (probability distribution of heights in CHMs, see section 3.1.1), which explained between 48% and 74% of bird diversity and abundance (*Figure 10.*, bottom row). Sites where the probability to find heights between 4.5 - 10 m is higher, presented lower diversity and abundance of birds (*Figure 10.*).

Figure 10

Scatter plot using the most related canopy structure variables with bird biodiversity.

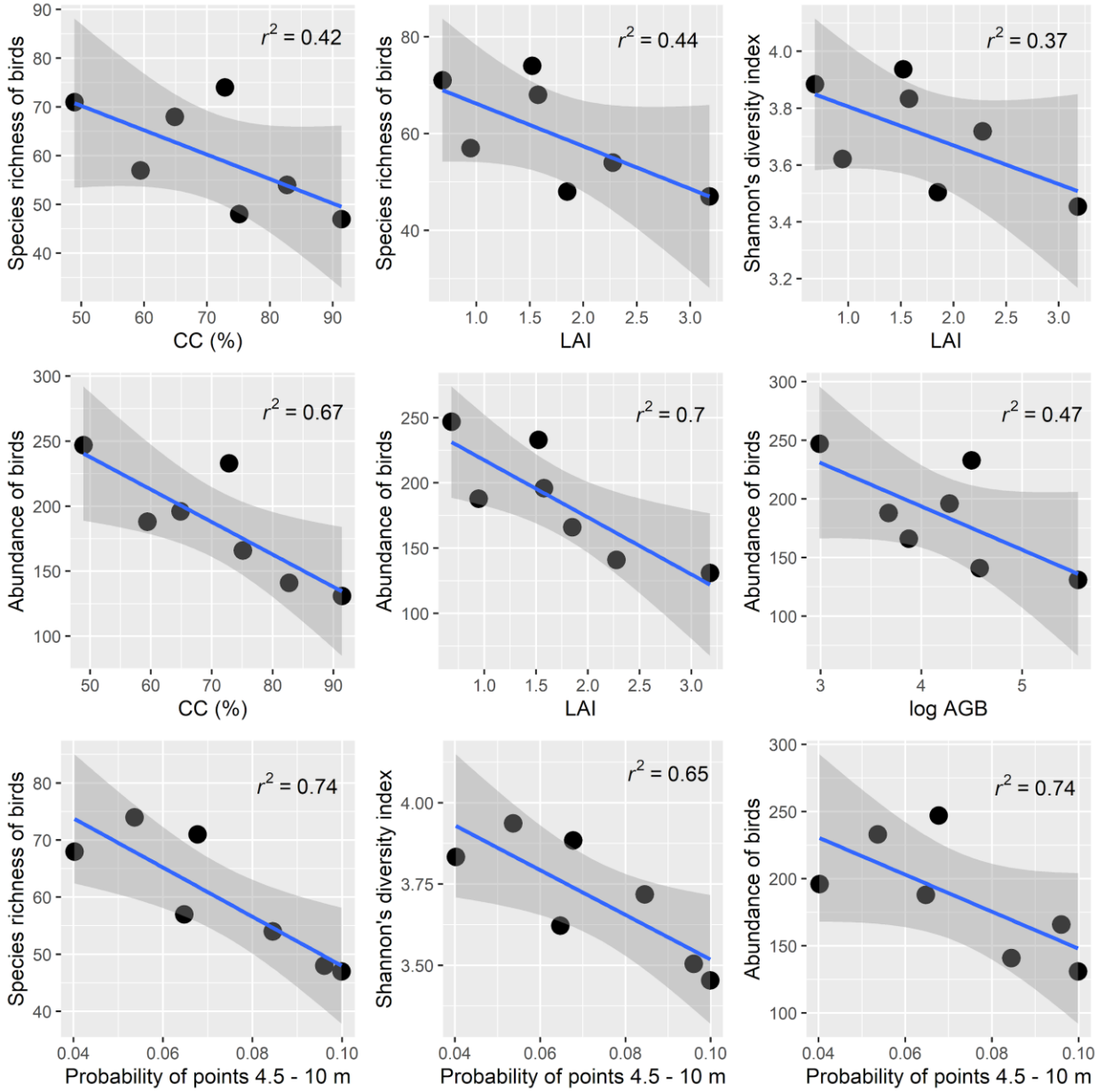

Note. Upper row) best relationships with bird biodiversity, Middle row) best relationships with bird abundance. On the bottom row, we show the major relationships between 3D variables (*s10_max*), richness, the Shannon's diversity index and abundance of birds.

Species composition is in contrast explained by different variables indicating the density and height distribution of the shade tree canopy layer (i.e. overstory) explaining the percentages between 40 and 64 percent of variation in species composition. In general, bird composition captured by *pcoa1* was mainly related to the intensity of space-filling, while *pcoa2* had strong relationships with variables related to the scale of space-filling (*Figure 11*.). For instance, *pcoa1* was highly correlated with density of shade trees *(D_over*, which is an indicator of the intensity of space-filling*)*, and *pcoa2* was mainly related to mean height and standard deviation of overstory (*H_over*, *H_sd_over*), canopy variables related to scale of space-filling . The highest correlation of bird composition with 3D variables was between *pcoa2* and percentage of canopy cover over 20 m (*s20*, explained 78% of the axis related with abundance of generalist species), followed by *pcoa2* with *glcm_contrast* (61% of variation explained) and *pcoa1* with *denq90* (which explained 44% of variation in bird composition).

Figure 11

Regression between bird composition, canopy structure and 3D variables.

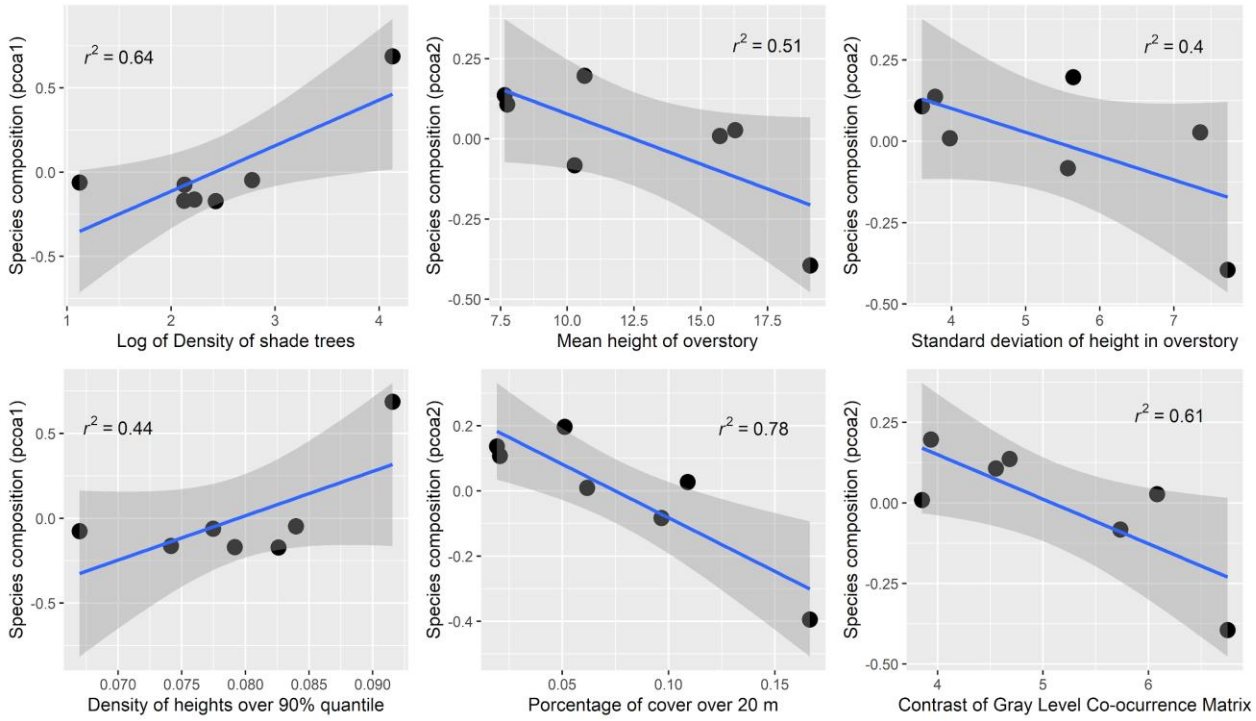

Note. Bird composition as revealed by the first axis of a Principal Coordinate analysis on species abundance), canopy structure variables (upper row) and 3D variables derived from SfM point-clouds (bottom row).

Principal Component Analysis between variables of canopy structure measured at site-level, 3D variables, species diversity and composition of the avifauna revealed the following relationship among variables: all vegetation structure variables were highly related with at least one 3D variable, moreover, birds biodiversity was related with at least one class of canopy structure variable or both (measurements on the ground and 3D variables, *Figure 12.*). Species richness and bird abundance decrease when variables related with intensity and scale of space-

filling (i.e. *D_over*, *AGB*, *LAI*, *CC*, *denq90*, *s10_med*, *s10_max*) increase, however the species composition also changes when decreasing species richness and bird abundance.

Figure 12

Principal component analysis with the most related variables with bird composition and biodiversity.

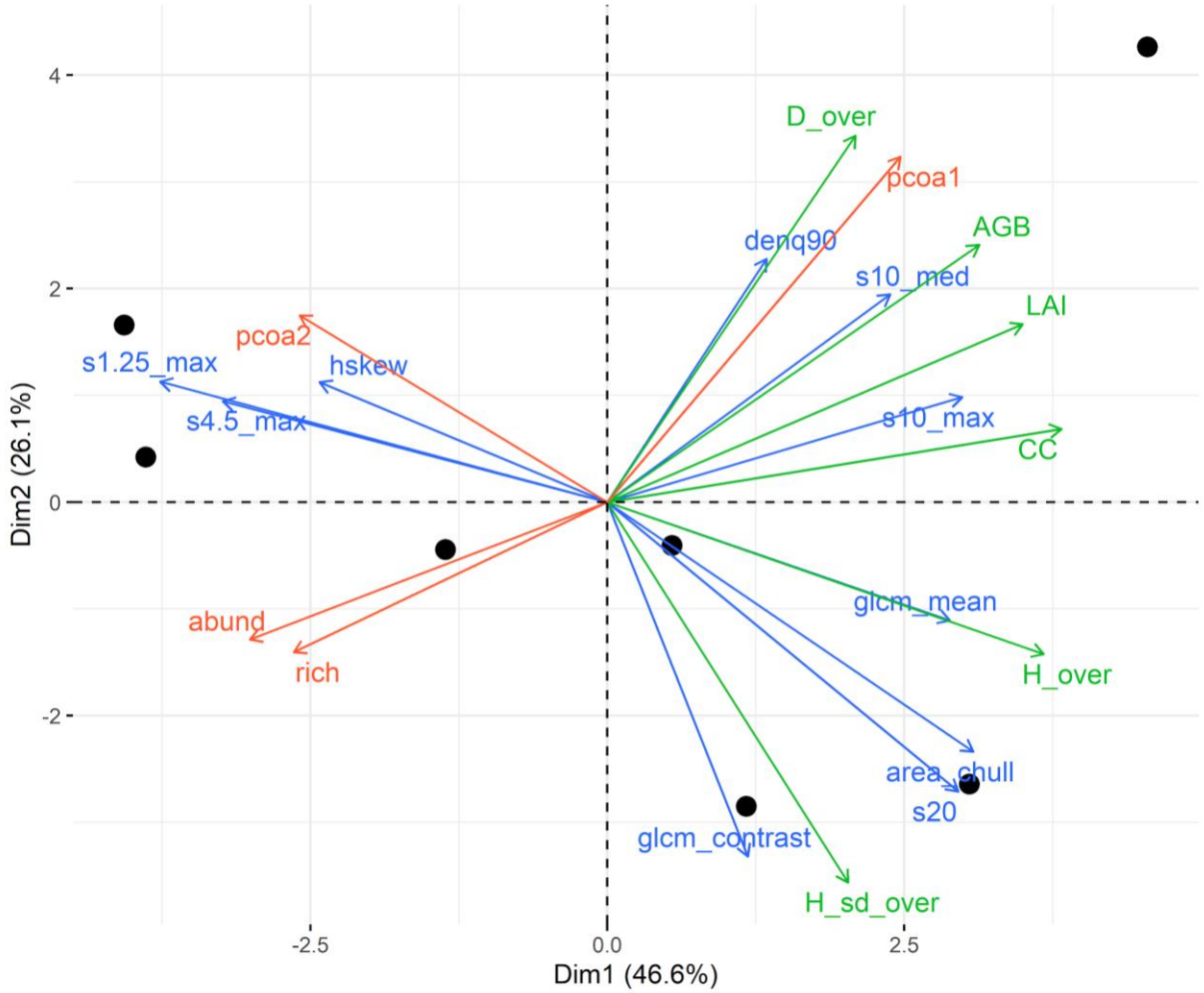

Note. PCA shows the correlation between canopy structure variables (green vectors), 3D variables derived from SfM point-clouds (blue vectors) and variables of bird biodiversity and species composition (derived from Principal Coordinate Analysis, pcoa, as red vectors) at the site-level.

4. Discussion

I was able to predict six important canopy structure variables (*LAI*, *CC*, *AGB*, *D_over*, *H_over* and *H_sd_over*) that can affect the space-filling of AFS using RGB images acquired with a drone, the SfM imaging technique and derived 3D variables. The predictions were more accurate at plot-level than at site-level, especially for variables related to the intensity of space-filling (*D_over* and *LAI*).

4.1. Performance of predictive models of canopy structure variables

Considering the relative root mean square error (RRMSE), the best predicted variable was *AGB* with a R^2 of 0.81 and 10% of RRMSE, followed by CC (R^2 = 0.82, RRMSE = 13%) and LAI (R^2 = 0.81, RRMSE = 24%). The predictive model for *AGB* without the inclusion of land-use type resulted in a R^2 of 0.58 and a RRMSE of 17% which is similar to the performance reported for the estimation of AGB in tropical woodlands (Kachamba et al., 2016). For AGB the inclusion of land-use type improved the performance of the final model, reducing the RRMSE by 7%. This indicates that some variation of canopy structure cannot be captured by variables derived from SfM point-clouds, most likely because of their limitation to penetrate into lower canopy layers. In addition, the estimation of AGB in tropical forests can be affected by multiple factors such as the accuracy of height determined by on-ground measurements, which may limit the reconstruction of SfM point-clouds in dense canopies (Laurin et al., 2019). Also, environmental conditions at the time of image acquisition, the number of matched images and overlap among images can affect the quality of point-clouds reconstructions. Although in this study I did not use Terrestrial Laser

Scanning (TLS) which has been recognized as the best ground-based method for characterizing the distribution of canopy biomass (Seidel et al., 2011). I demonstrated that it is possible to generate accurate results using a low-cost methodology. The final predictive model for AGB had similar values of R^2 and RMSE compared to previous studies considering site-specific as well as global calibration (Zahawi et al., 2015).

Predictions for LAI were of similar or even better performance that the one reported on other studies, even without land-use type inclusion. For example, LAI has been predicted in a temperate riparian forest with a R^2 of 0.62 and a RMSE of 0.4, using percentiles of heights (at 40% and 95%) and the shape of the probability distribution of height values, as predictors (Axe, 2018). I also found that the predictive model of *LAI* included variables related to the probability distribution of heights (i.e. *denq75*, *s1.25_max* and *s4.5_sd*). My predictions for *LAI*, *CC* and *AGB*, which include the density of heights above the 75% percentile (*denq75*) showed higher R^2 and lower RMSE compared to predictions of LAI by Zhang et al. (2019) where they also used as predictors quartiles of the height distribution in CHMs (*RH25, RH50, RH75* and *RH100*). In addition, a study estimated the overstory canopy cover (*CC*) in forest plantations from China with a R^2 of 0.52 but a similar RMSE = 0.12 (Li et al., 2020). This may be due to the fact that the canopy structural gradient investigated here is more pronounced (i.e. from low canopy cover of AFS to dense forest) as compared to the canopy structural gradients in other studies (e.g. forest plantation or forest). Nevertheless, in the context of AFS with coffee and cacao, the results highlight that AGB, CC and LAI as indicators for management and key ecosystem characteristics can be well derived using low-cost drone remote sensing.

In mountainous tropical forests the accuracy for predictions of canopy height has been successful using SfM-derived CHMs as well as lidar-derived CHMs (Chung et al., 2019), despite

the continuous tree canopy layer. Although my predictions of the heights of shade trees in the canopy (*H_over*) had good adjustment ($R^2 = 0.82$), it showed a substantial lower R^2 and higher error rate, as compared for example to the dominant height predicted by Puliti et al. (2015). This difference could be generated by two main reasons, 1) the less accurate DTM, derived from lowest points in SfM point-clouds because the study area is located in a mountainous region, 2) the low accuracy of height in GCPs can generate systematic errors in CHMs, since they were taken using the waypoint averaging function of handheld GPS instead of Differential Global Positioning System (DGPS), which is slightly more accurate on the Z-axis (height measurement) (Benassi et al., 2017). However, predictions of mean canopy height in other tropical forests in Indonesia have been successful using information derived from SfM point-clouds, even without the inclusion of GCPs information (Swinfield et al., 2019). In my study, the gradient of canopy cover is large (many AFS have a discontinuous canopy layer, because of the low density of shade trees), therefore it was possible to make good characterization of canopy height in low dense canopy crops as AFS with coffee using SfM point-clouds.

SfM point-cloud reconstructions in tropical and temperate forests have shown to capture little information at ground-level in dense canopies (Wallace et al., 2016; Roşca et al., 2018; Swinfield et al., 2019) and this is one of the main concerns to characterize midstory vegetation. In my case, since low shade AFS do not have dense canopies the SfM reconstructions were able to capture some information at low canopy heights. Therefore, the forests showed higher probability of heights over 4.5 m while in AFS with coffee showed higher probabilities under 1.25 m (*Figure 7.*). Recently Giannetti et al. (2018) proposed the use of DTM-independent variables to avoid the need for an accurate DTM to derive CHMs. In order to predict mean value and standard deviation of height in tallest trees, Giannetti et al. (2020) included in their models homogeneity (i.e. a textural

feature), percentile of 70% of heights as well as the proportion of points over 30% and 70% percentiles (d3, d7) but these models presented a lower R^2 and accuracy compared to my results. Hence, the generation of DTM based on the lowest points of SfM point-clouds reveals that (like my approach), could improve results of prediction using multiple linear models.

In this study, the prediction of the density of trees in the overstory *D_over* (34% of RRMSE with a mean of 15.14 trees per 900 m^2) also known as Stem number (S_n) was similar to their estimation using metrics derived directly from DSM (Puliti et al., 2019). However, the most important variables used by Puliti et al. (2019) such as glcm second_moment, 10% percentile, min, max and median of DSM were different from those used in my model. This suggests that different sources of information (CHM instead of DSM) affect the selection of predictor variables, and DTM reconstruction has an impact over minimum and maximum values registered in the CHMs. Stem number is a little explored variable in this kind of studies (Guimarães et al., 2020) and has usually lower correlations with predictors than those found for DBH, AGB and height variables (Cao et al., 2019). Even if the prediction is based on airborne lidar information the number of trees per plot has been associated with big errors in dense covers, despite their ability to derive information under the canopy layer (Gobakken & Næsset, 2004). Nevertheless, it is an important variable to predict in the context of AFS, because the presence of trees decreases erosion and is linked with soil conservation (Meylan et al., 2017). Overall, the best models (i.e. with the lowest AIC) at the site-level (i.e. aggregation of several plots at a site), showed higher RRMSE than those found at the plot-level. This result contradicts the findings by Puliti et al. (2019), where stand (or site) level models performed better than plot-level models, probably due to the reduction of extreme observations because of site level averaging. In this study, I found that the site level models predicted *D_over* and *LAI* less well, which can be related with differences in the number of plots

aggregated by site, high variation of 3D variables between plots belonging to the same site, and also the error induced by the inclusion of canopy trees that were not measured on the field.

4.2. Variable importance of 3D predictors

3D variables related to the intensity of space-filling (density of height over 75% and 90% percentiles, *denq75* - *denq90*) were the most important predictors of *D_over*, *CC* and *logAGB* (see Table 5. and Table 6.). For example, d*enq90* along with variation in the probability distribution of heights between 4.5 - 10 m (*s10_sd*) were positively correlated with *D_over*, which indicates that a high number of values over 90% quantile or between 4.5 - 10 m are indicators of a higher intensity of canopy space-filling, CC is positively correlated with *denq75* and *VCIsd*, which indicates that the number of values of height over 75% quantile and a higher variation in the distribution of heights are related to a dense canopy cover. *AGB* was positively correlated with *denq75* and median of the probability distribution of heights between 1.25 - 4.5 m (*s4.5_med*), which indicates that the presence of higher number of values over 1.25 m and 75% quantile in the CHM is related with higher amounts of biomass. The best model for *AGB* was the only one which included textural features: *glcm_contrast* and *glcm_second_moment* (also called energy). Texture variables extracted from a height raster of the canopy have not been used in other studies for the prediction of above-ground biomass; this is an important result since its inclusion increases R^2 and decreases RRMSE.

Canopy variables related to the scale of space-filling (*LAI*, *H_over* and *H_sd_over*) were mainly determined by 3D variables based on canopy heights and their vertical distribution (*VCIsd*, *denq75* and *s4.5_sd*). Though vertical complexity index (VCI) was initially proposed as a metric

derived from lidar points-clouds (van Ewijk et al., 2011), in this study *VCIsd* based on SfM point-clouds proved to be useful for *LAI*, and *H_sd_over* predictions. Prediction of *LAI* was mainly determined by *VCIsd* and *denq75*, which were positively correlated to the dependent variable. The prediction of *H_over* was negatively related to *s4.5_sd*, which indicates that areas with a low density of values between 1.25 - 4.5m, usually have a higher mean canopy height. On the other hand, *H_sd_over* was positively correlated with *VCIsd*, *COVAR and Q10*, demonstrating the utility of these 3D variables (which characterize the distribution of heights) for prediction of the scale of space-filling.

Variables based on the probability distribution of heights (also related to scale of space-filling) such as *s4.5_sd* and *s1.25_max* represent an useful source of information for prediction of almost all canopy structure variables except for *H_sd_over*. The *s4.5_sd* had negative coefficients in final models of *LAI*, *CC*, *AGB* and *H_over*, which indicates that a high probability to find heights (in CHMs) between 1.25 - 4.5 m is related with low canopy cover (*CC*) and smaller amounts of above-ground biomass (*AGB*). This pattern can be due to the occupation of a large part of the lower canopy area by cacao or coffee crops (compared to saplings in forest), reducing the availability of space to find tall shade trees. At the plot-scale the surface area of the convex hull (*area_chull*) was also identified as an important variable for predictions of *D_over* and *H_over*. This has not been reported in previous works using a plot-based approach, but my result shows that an increase in the surface of point-clouds can indicate high numbers of trees and high variation of heights in shade trees. The coefficient of variation of heights (*COVAR*) was useful to predict *CC* and *H_sd_over*, although *COVAR* has been used for the characterization of maize, aquatic plants and vineyards. Only the study of Axe (2018) used it to predict LAI in riparian forests. This highlights

the importance of the aforementioned 3D variables to predict both intensity and scale of canopy space-filling.

Previous works showed that the most important SfM point-cloud derived predictors for canopy structure have been related to height measurements as percentiles of heights. For example, Ota et al. (2017) found that 90% percentile (h_{90}) of CHMs was the most important variable to estimate mean height. For LAI the percentile of 95% (P95) combined with the coefficient of variation (CV) were significant predictors (Axe, 2018). In addition, prediction of AGB (using multiple linear regression) in tropical woodlands showed that the most useful SfM point-cloud metrics were *Hmax, H30* (30% percentile), *D0, D1, D2* (Proportion of points above 0, 10 and 20% percentile) and variance of height - *Hvariance* (Kachamba et al., 2016; Domingo et al., 2019).

Model performance and predictor variables varied for the majority of response variables between plot and site-level (Table 3 and Table 4). The best predictive models for canopy structure at the site-level (i.e. farm or cultivation) obtained higher R^2 than the models fitted at plot-level. Nevertheless, at site-level the RRMSE also increased, which indicates an increase in model bias. For example, *LAI* was predicted by *denq90,* and the area of the convex hull (*area_chull*), variables that were not included in the *LAI* model at plot-level. However, *denq90* is highly related to *denq75,* and the latter was important for prediction of *LAI, CC* and *AGB* at plot-level. This indicates that similar 3D information was important for accurate predictions; however, the redundancy of information among the many 3D variables resulted in 'switching' predictors. Best models for *CC* and *AGB* at site-level also changed *denq75* for *denq90,* including *s1.25_max* and *area_chull,* respectively. *D_over* prediction at the site-level also included *denq90, denq75* and *VCIsd* as predictors, however the relative RMSE was higher than 100%, which indicates the loss of the models' ability to predict density of shade trees (*D_over*) at the site-level. Therefore, I suggest for

future studies the use of an approach at the plot-level. In this study, the aggregation to the site-level was only done to allow the evaluation of the impact of canopy structure on avian diversity and composition (see section 5.5.). For *H_over* the best model included *s4.5_med*, which is highly related to *s4.5_sd*, an important predictor variable at plot-scale. On the other hand, *area_chull* was not selected for the best model at site-level and instead the 10% quantile (*Q10*) and the proportion of cover by pixels over 30 m (*s30*) were selected. Finally, the coefficient of variation of heights (*COVAR)* and the maximum height in CHM (*hmax)* were retained for the best model of *H_sd_over* at site-level. Predictors seem to change according to spatial scale, however variables from the best models at the site-level seem to maintain a close relationship with their counterparts at plot-level.

4.3. Space-filling of canopy across land-use types

Forest showed to have higher intensity of space-filling than AFS, based on higher values of *LAI* and *CC* at the upper canopy, as well as higher, *AGB* and *D_over* in general (*Figure 9.*). On the other hand, the scale of space-filling did not differ between forest and AFS, since some AFS plots exceeded the average height (*H_over*) and the variation of heights (*H_sd_over*) found in forest plots. These results highlight the importance of complex structure in AFS where high trees and a high variation in heights are similar to intact forest areas.

The inclusion of land-use type as an additive term (a not interaction term) in the multiple linear regression model resulted in significant improvements for prediction of all canopy structure variables. This indicates differences in canopy structure (or architecture) between land-use types that cannot be captured by the 3D variables generated in this study. This might be caused by an insufficient characterization of the midstory by those metrics because of the limitations of SfM

point-clouds to capture aspects of the lower canopy. Nevertheless, metrics such as *denq90, VCIsd* and the probability distributions of heights (*s1.25_max, s4.5_sd and s10_sd*) in CHMs can help to include specific features of each land-use type and estimate canopy structure variables successfully.

Variables derived from digital aerial photogrammetry point-clouds can help to characterize vertical and horizontal canopy structure in temperate forests (Jayathunga et al., 2019). Nevertheless, they seem to better predict features related with canopy height (scale of space-filling) rather than variables related to the intensity of space-filling (Noordermeer et al., 2019). Those studies also demonstrate that forest canopy structure classes (i.e. young forest, low productivity and high productivity forest) are important for predictions and can be characterized based on those 3D metrics. However, temperate forests are composed of fewer species than tropical forests that have many plant species and many different growth forms. Fortunately, it is possible to relate land-use type with 3D variables derived from SfM point-clouds, because human interventions can generate an unique 3D vegetation structure (Guo et al., 2017), which is also the case for AFS (i.e. AFS with coffee having a higher intensity of space-filling at the lower canopy than AFS with cacao). Moreover, potential areas where national Corine Land Cover classification has identified cacao crops, coffee plantations and dense natural forest can be used as targets to apply the predictive models presented here. UAVs have higher potential to include in the monitoring and management of biodiversity-friendly agricultural landscapes (Librán-Embid et al., 2020) and SfM point-clouds has been seen as an optimal tool for 3D mapping of ecosystems in the new era of spatial ecology (D'Urban Jackson et al., 2020).

4.4. Space-filling as driver of bird diversity and species composition

Bird species richness and Shannon's diversity index was strongly correlated to *AGB, LAI*, *CC* and probability distribution of heights between 4.5 - 10 m (*s10_max*). The relationships were negative, which indicates that the most biodiversity sites were identified as AFS with low above-ground biomass and low canopy cover over 4.5 m. This can be influenced by landscape metrics as proximity to forest but also to an underestimation of the true diversity of birds in the forest. The latter may be due to the low conditions of detectability of bird species through observation in dense covers or the low availability of food resources during time of sampling. Thus, I recommend sampling the diversity of organisms at different times of the year, in order to generate better diversity estimation comparable between land-use types and to the variables derived from the SfM point-clouds.

I also found a good but negative relationship between *CC*, *LAI*, *AGB* and bird abundances, where sites with the highest *CC* and *AGB* showed the lowest bird abundance. These results differ from other neotropical AFS studies (Philpott & Bichier, 2012) where the abundance of birds was higher in the forest. The lowest abundance of birds was found in forest but also increased in AFS according to the canopy shade. The data showed that bird composition changes drastically between forests and AFS, with more specialists in forest but generalist and more abundant species reported in crops, which was also reported by Harvey & González Villalobos (2007). This pattern and the higher abundance of birds in AFS with high shade can be due to the presence of trees of Fabaceae family members on farms which increase the visit of insectivorous bird species (Narango et al., 2019).

Although I did not find a good relationship between *D_over*, *H_sd_over* and bird abundances, bird composition (*pcoa1* and *pcoa2*) registered the strongest correlation with *D_over*, *LAI*, *AGB* and with 3D variables related to intensity and scale of space-filling (*denq90*, *s20* and *glcm_contrast*, see Figure 11.). In my study the relative RMSE of *D_over* prediction at site level was over 100% which indicates a limitation of 3D variables to predict this important feature for bird diversity at larger scales. Studies in tropical regions have found a positive relationship between abundances of birds and higher complexity in vertical structure (Mahiga et al., 2019). In 2004 Naidoo found that high vertical heterogeneity was related to presence of specialists instead of generalist species, but these dynamics can be influenced by landscape metrics as the proximity to intact forest patches (Laube et al., 2008). Canopy structure variables such as tree density (Naidoo, 2004) and vertical vegetation heterogeneity (Laube et al., 2008) have shown great influence over bird composition. For this reason, knowing the number of trees per area and the canopy height will help to guide sustainable management for bird conservation.

Multiple sources of errors can influence the prediction of canopy structure at site-level and therefore relationships of SfM-derived variables with fauna inventories should be taken with caution. For example, plant species diversity and composition in tropical AFS is an important factor which affects bird species diversity (Perfecto et al., 2004), however I did not evaluate plant composition in forest plots and thus I cannot evaluate the influence of trees biodiversity over the reported bird abundances.

The good relationships between canopy structure and variables derived from SfM point-clouds suggests that 3D information obtained with processing of UAV aerial images can be used as training data for satellite information (Kato et al., 2015). For instance, the Global Ecosystem Dynamics Investigation (GEDI) which seeks to characterize 3D forest structure using a LIDAR

full-waveform needs a calibration - validation (cal/val) procedure (Dubayah et al., 2020) that could be done using SfM information. In addition, this information could also help to improve accuracy of global, regional, and national monitoring schemes which seek for Essential Biodiversity Variables (EBV) (Proença et al., 2017). In a few words, it is important to characterize (agro)forest structure using RS because it can help to monitor the reduction in the complexity of canopy structure (Dupuis et al., 2020; Bourgoin et al., 2020), recovery (Zahawi et al., 2015) and disasters in tropical forests (Kato et al., 2017). Using the approach presented here I was able to characterize AFS space-filling and I showed that it is related to bird species diversity and composition. This shows on the one hand that we can monitor 3D canopy architecture of AFS in a cheap manner and that it is relevant for bird habitat structure. In other words, 3D variables acquired with drones can serve as EBV and also as potentially mapped from space (i.e. GEDI).

5. Conclusions

In this study, by using variables derived from SfM point-clouds, I showed that the intensity of space-filling is higher in forest than in AFS, while its scale did not differ between both land-use types. Traditional field data acquisition can be successfully used as ground truth data to develop predictive models using variables derived from SfM point-clouds, even using low-cost equipment and sensors (i.e. handheld GPS, low-cost RGB camera) and in rough terrain. Multiple linear regression with variable selection and cross-validation can predict canopy structure variables related to the space-filling (*LAI*, *CC*, *AGB*, *D_over*, *H_over* and *H_sd_over*) with high accuracy and low error rates. The prediction of canopy structure variables improved significantly when including land-use type, which indicates a limitation of this approach, potentially related to the

limited characterization of the low canopy. Finally, applying the concept of space-filling to predict habitat quality for birds highlights its importance for the estimation of habitat complexity. This gives avenue to use it as an essential biodiversity variable, which allows the recognition of the biodiversity conservation potential of Andean agro-ecosystems.

6. Recommendations

In mountain regions many sources of error appear to impact 3D models reconstruction from SfM point-clouds, such as the light conditions, the slope, weather conditions as well as geometrical properties of the canopy (Rahlf et al., 2017). For this reason, it is important to take into consideration these parameters in the planification of flight plans, image acquisition and processing. Spectral information represents an opportunity to include species-specific information (Puliti et al., 2019) and has shown to be useful for land cover classification (De Luca et al., 2019). Thus, the inclusion of spectral information (e.g. using multispectral cameras such as the Micasense RedEdge-MX) can enhance predictions of canopy structure which depends on land-use type. However, in tropical regions where many land-use types consist of diverse species mixtures, the incorporation of spectral data faces other challenges, such as the radiometric calibration in aerial photographs. I recommend the use of ethylene-vinyl acetate as reference panels for reflectance calibration (Jeong et al., 2018), in order to make measurements of different flights comparable between them (Packalén & Maltamo, 2007). But also if it is possible, and the budget of research allows it, I suggest the use of a terrestrial laser scanning, the incorporation of a high precision GPS device to GCPs measurements and the use of a light sensor which can help to improve calibration of reflectance.

The use of information extracted from drone images can enrich future research in biodiversity conservation and ecological monitoring (Díaz-Delgado & Mücher, 2019). Aerial images have a high number of applications, for example, the mapping of ecosystem services and EBV's, delineation of organisms (i.e. between trees and shrubs, as well as between species) and even upscaling ecological variables from drone to satellite images (e.g. Sentinel 2). Therefore, I recommend the use of variables extracted from SfM point-clouds which can help to describe canopy structure and variables related with fauna biodiversity, for future studies where species distributions or habitat suitability is the objective. These studies also can be interesting to understand differences of the relationships between canopy structure complexity and biodiversity for different faunistic groups.

References

Agisoft, L. L. C., & St Petersburg, R. (2019). Agisoft metashape. *Professional Edition*, *7*. web site. Available: http://www.agisoft.com. [Accessed August 17, 2020]

Albrecht, A., & Kandji, S. T. (2003). Carbon sequestration in agroforestry systems. *Agriculture, Ecosystems & Environment*, *99*(1–3), 15–27. https://doi.org/10.1016/S0065-2113(10)08005-3

Alvarez, E., Duque, A., Saldarriaga, J., Cabrera, K., De, G., Lema, A., … Rodríguez, L. (2012). Forest Ecology and Management Tree above-ground biomass allometries for carbon stocks estimation in the natural forests of Colombia. *Forest Ecology and Management*, *267*, 297–308. https://doi.org/10.1016/j.foreco.2011.12.013

Asare, R., Afari-Sefa, V., Osei-Owusu, Y., & Pabi, O. (2014). Cocoa agroforestry for increasing forest connectivity in a fragmented landscape in Ghana. *Agroforestry Systems*, *88*(6), 1143–1156. https://doi.org/10.1007/s10457-014-9688-3

Axe, T. (2018). *Leaf Area Index in Riparian Forests: Estimation with Airborne Lidar vs. Airborne Structure-from-Motion and the Societal Value of Remotely Sensed Ecological Information* (Doctoral dissertation).

Bagaram, M. B., Giuliarelli, D., Chirici, G., Giannetti, F., & Barbati, A. (2018). UAV remote sensing for biodiversity monitoring: Are forest canopy gaps good covariates? *Remote Sensing*, *10*(9), 1–28. https://doi.org/10.3390/rs10091397

Bakermans, M. H., Rodewald, A. D., Vitz, A. C., & Rengifo, C. (2012). Migratory bird use of shade coffee: The role of structural and floristic features. *Agroforestry Systems*, *85*(1), 85–94. https://doi.org/10.1007/s10457-011-9389-0

Benassi, F., Dall'Asta, E., Diotri, F., Forlani, G., Morra di Cella, U., Roncella, R., & Santise, M. (2017). Testing accuracy and repeatability of UAV blocks oriented with GNSS-supported aerial triangulation. *Remote Sensing*, *9*(2), 172.

Bhagwat, S. A., Willis, K. J., Birks, H. J. B., & Whittaker, R. J. (2008). Agroforestry: a refuge for tropical biodiversity? *Trends in Ecology and Evolution*, *23*(5), 261–267. https://doi.org/10.1016/j.tree.2008.01.005

Bosselmann, A. S., Dons, K., Oberthur, T., Olsen, C. S., Ræbild, A., & Usma, H. (2009). The influence of shade trees on coffee quality in small holder coffee agroforestry systems in Southern Colombia. *Agriculture, Ecosystems and Environment*, *129*(1–3), 253–260. https://doi.org/10.1016/j.agee.2008.09.004

Bourgoin, C., Betbeder, J., Couteron, P., Blanc, L., Dessard, H., Oszwald, J., ... & Sist, P. (2020). UAV-based canopy textures assess changes in forest structure from long-term degradation. *Ecological Indicators*, *115*, 106386.

Brüning, L. Z., Krieger, M., Meneses-Pelayo, E., Eisenhauer, N., Ramirez Pinilla, M. P., Reu, B., & Ernst, R. (2018). Land-use heterogeneity by small-scale agriculture promotes amphibian diversity in montane agroforestry systems of northeast Colombia. *Agriculture, Ecosystems and Environment*, *264*(May), 15–23. https://doi.org/10.1016/j.agee.2018.05.011

Cao, L., Liu, H., Fu, X., Zhang, Z., Shen, X., & Ruan, H. (2019). Comparison of UAV LiDAR and digital aerial photogrammetry point clouds for estimating forest structural attributes in subtropical planted forests. *Forests*, *10*(2), 145.

Chang, W. C., Wu, C. H., Tsai, Y. H., & Chiu, W. Y. (2018). Object volume estimation based on 3D point cloud. *2017 International Automatic Control Conference, CACS 2017*, *2017–November*, 1–5. https://doi.org/10.1109/CACS.2017.8284244

Chung, C. H., Wang, C. H., Hsieh, H. C., & Huang, C. Y. (2019). Comparison of forest canopy height profiles in a mountainous region of Taiwan derived from airborne lidar and unmanned aerial vehicle imagery. *GIScience & Remote Sensing*, *56*(8), 1289-1304.

Deheuvels, O., Avelino, J., Somarriba, E., & Malezieux, E. (2012). Vegetation structure and productivity in cocoa-based agroforestry systems in Talamanca, Costa Rica. *Agriculture, Ecosystems and Environment*, *149*, 181–188. https://doi.org/10.1016/j.agee.2011.03.003

Deheuvels, O., Rousseau, G. X., Quiroga, G. S., Franco, M. D., Cerda, R., Mendoza, S. J. V., & Somarriba, E. (2014). Biodiversity is affected by changes in management intensity of cocoa-based agroforests. *Agroforestry Systems*, *88*(6), 1081–1099. https://doi.org/10.1007/s10457-014-9710-9

De Luca, G., N Silva, J. M., Cerasoli, S., Araújo, J., Campos, J., Di Fazio, S., & Modica, G. (2019). Object-based land cover classification of cork oak woodlands using UAV imagery and orfeo toolbox. *Remote Sensing*, *11*(10), 1238.

Díaz-Bohórquez, A. M., Bayly, N. J., Botero, J. E., & Gómez, C. (2014). Aves migratorias en agroecosistemas del norte de Latinoamérica , con énfasis en Colombia Perspectivas en Ornitología Colombiana. *Ornitología Colombiana*, *14*, 3–27.

Díaz-Delgado, R., & Mücher, S. (2019). Editorial of Special Issue "Drones for Biodiversity Conservation and Ecological Monitoring".

Domingo, D., Ørka, H. O., Næsset, E., Kachamba, D., & Gobakken, T. (2019). Effects of uav image resolution, camera type, and image overlap on accuracy of biomass predictions in a tropical woodland. *Remote Sensing*, *11*(8), 948.

Dubayah, R., Blair, J. B., Goetz, S., Fatoyinbo, L., Hansen, M., Healey, S., ... & Armston, J. (2020). The Global Ecosystem Dynamics Investigation: High-resolution laser ranging of the

Earth's forests and topography. *Science of Remote Sensing, 1*, 100002.

Dupuis, C., Lejeune, P., Michez, A., & Fayolle, A. (2020). How Can Remote Sensing Help Monitor Tropical Moist Forest Degradation?—A Systematic Review. *Remote Sensing*, *12*(7), 1087.

D'Urban Jackson, T., Williams, G. J., Walker-Springett, G., & Davies, A. J. (2020). Three-dimensional digital mapping of ecosystems: a new era in spatial ecology. *Proceedings of the Royal Society B*, *287*(1920), 20192383.

Frey, J., Kovach, K., Stemmler, S., & Koch, B. (2018). UAV Photogrammetry of Forests as a Vulnerable Process. A Sensitivity Analysis for a Structure from Motion RGB-Image Pipeline. Remote Sensing, 10(6), 912.

Fromm, V. (2019). Bird diversity and composition along a management gradient in a heterogeneous agroforest landscape in the Northern Andes of Colombia (Master's thesis, Universität Leipzig, Leipzig, Germany).

Garrity, D. P. (2006). World agroforestry into the future. World Agroforestry Centre.

Gatti, F. D., Rodrigues, T. H. A., Figueiredo, L. A. D., & Carneiro, M. A. A. (2018). Longhorn Beetle (Coleoptera: Cerambycidae) Assemblage and the Structural Heterogeneity of Habitat at the Brazilian Atlantic Forest. *Environmental Entomology*, *47*(6), 1413–1419. https://doi.org/10.1093/ee/nvy158

Giannetti, F., Chirici, G., Gobakken, T., Næsset, E., Travaglini, D., & Puliti, S. (2018). A new approach with DTM-independent metrics for forest growing stock prediction using UAV photogrammetric data. *Remote Sensing of Environment*, *213*, 195-205.

Giannetti, F., Puletti, N., Puliti, S., Travaglini, D., & Chirici, G. (2020). Assessment of UAV photogrammetric DTM-independent variables for modelling and mapping forest structural

indices in mixed temperate forests. *Ecological Indicators, 117*, 106513.

Gobakken, T., & Næsset, E. (2004). Estimation of diameter and basal area distributions in coniferous forest by means of airborne laser scanner data. *Scandinavian Journal of Forest Research*, *19*(6), 529-542.

Guevara-Escobar, A., Tellez, J., & Gonzalez-Sosa, E. (2005). Use of digital photography for analysis of canopy closure. *Agroforestry Systems*, *65*(3), 175–185. https://doi.org/10.1007/s10457-005-0504-y

Guimarães, N., Pádua, L., Marques, P., Silva, N., Peres, E., & Sousa, J. J. (2020). Forestry Remote Sensing from Unmanned Aerial Vehicles: A Review Focusing on the Data, Processing and Potentialities. *Remote Sensing*, *12*(6), 1046.

Guo, X., Coops, N. C., Tompalski, P., Nielsen, S. E., Bater, C. W., & Stadt, J. J. (2017). Regional mapping of vegetation structure for biodiversity monitoring using airborne lidar data. *Ecological informatics, 38*, 50-61.

Günlü, A., & Kadiogullari, A. I. (2018). Modeling forest stand attributes using Landsat ETM+ and QuickBird satellite images in western Turkey. *Bosque (Valdivia), 39*(1), 49–59. https://doi.org/10.4067/s0717-92002018000100049

Hall, R. J., Skakun, R. S., Arsenault, E. J., & Case, B. S. (2006). Modeling forest stand structure attributes using Landsat ETM+ data: Application to mapping of aboveground biomass and stand volume. *Forest Ecology and Management*, *225*(1–3), 378–390. https://doi.org/10.1016/j.foreco.2006.01.014

Haralick, R. M., Shanmugam, K., & Dinstein, I. H. (1973). Textural features for image classification. *IEEE Transactions on systems, man, and cybernetics*, (6), 610-621.

Harvey, C. A., & González Villalobos, J. A. (2007). Agroforestry systems conserve species-rich

but modified assemblages of tropical birds and bats. *Biodiversity and Conservation*, *16*(8), 2257–2292. https://doi.org/10.1007/s10531-007-9194-2

Hernández-Vasquez, E., Campos-Ángeles, G., Enríquez-Del Valle, J., Rodrígues-Ortiz, G., & Velasco-Velasco, V. (2012). Captura de carbono por Inga jinicuil Schltdl. en un sistema agroforestal de café bajo sombra [Carbon sequestration on Inga Jinicuil Schltdl. in a shade coffee agroforestry system]. *Revista Mexicana de Ciencias Forestales*, *3*(9), 11–21. Retrieved from http://www.scielo.org.mx/pdf/remcf/v3n9/v3n9a2.pdf

Iglhaut, J., Cabo, C., Puliti, S., Piermattei, L., O'Connor, J., & Rosette, J. (2019). Structure from motion photogrammetry in forestry: A review. *Current Forestry Reports, 5*(3), 155-168.

Jayathunga, S., Owari, T., & Tsuyuki, S. (2019). Digital Aerial Photogrammetry for Uneven-Aged Forest Management: Assessing the Potential to Reconstruct Canopy Structure and Estimate Living Biomass. *Remote Sensing*, *11*(3), 338. https://doi.org/10.3390/rs11030338

Jeong, Y., Yu, J., Wang, L., Shin, H., Koh, S. M., & Park, G. (2018). Cost-effective reflectance calibration method for small UAV images. *International Journal of Remote Sensing*, *39*(21), 7225-7250.

Jiménez-Pérez, A., Cach-Pérez, M. J., Valdez-Hernández, M., & de la Rosa-Manzano, E. (2019). Effect of canopy management in the water status of cacao (Theobroma cacao) and the microclimate within the crop area. *Botanical Sciences*, *97*(4), 701-710.

Jose, S. (2009). Agroforestry for ecosystem services and environmental benefits: An overview. *Agroforestry Systems*, *76*(1), 1–10. https://doi.org/10.1007/s10457-009-9229-7

Juchheim, J., Ammer, C., Schall, P., & Seidel, D. (2017). Canopy space filling rather than conventional measures of structural diversity explains productivity of beech stands. *Forest Ecology and Management, 395*, 19-26.

Kachamba, D., Ørka, H., Gobakken, T., Eid, T., & Mwase, W. (2016). Biomass Estimation Using 3D Data from Unmanned Aerial Vehicle Imagery in a Tropical Woodland. *Remote Sensing*, *8*(11), 968. https://doi.org/10.3390/rs8110968

Kashung, Y., Das, B., Deka, S., Bordoloi, R., Paul, A., & Tripathi, O. P. (2018). Geospatial technology based diversity and above ground biomass assessment of woody species of West Kameng district of Arunachal Pradesh. *Forest Science and Technology*, *14*(2), 84–90. https://doi.org/10.1080/21580103.2018.1452797

Kato, A., Obanawa, H., Hayakawa, Y., Watanabe, M., Yamaguchi, Y., & Enoki, T. (2015, July). Fusion between UAV-SFM and terrestrial laser scanner for field validation of satellite remote sensing. In *2015 IEEE International Geoscience and Remote Sensing Symposium (IGARSS)* (pp. 2642-2645). IEEE.

Kato, A., Wakabayashi, H., Hayakawa, Y., Bradford, M., Watanabe, M., & Yamaguchi, Y. (2017, July). Tropical forest disaster monitoring with multi-scale sensors from terrestrial laser, UAV, to satellite radar. In *2017 IEEE International Geoscience and Remote Sensing Symposium (IGARSS)* (pp. 2883-2886). IEEE.

Koh, L. P., & Wich, S. A. (2012). Dawn of drone ecology: low-cost autonomous aerial vehicles for conservation. *Tropical conservation science*, *5*(2), 121-132.

Korhonen, L., Ali-Sisto, D., & Tokola, T. (2015). Tropical forest canopy cover estimation using satellite imagery and airborne lidar reference data. *Silva Fennica*, *49*(5). https://doi.org/10.14214/sf.1405

Krauss, J., Klein, A. M., Steffan-Dewenter, I., & Tscharntke, T. (2004). Effects of habitat area, isolation, and landscape diversity on plant species richness of calcareous grasslands. *Biodiversity and Conservation*, *13*(8), 1427–1439.

https://doi.org/10.1023/B:BIOC.0000021323.18165.58

Laube, I., Breitbach, N., & Böhning-Gaese, K. (2008). Avian diversity in a Kenyan agroecosystem: effects of habitat structure and proximity to forest. *Journal of Ornithology*, *149*(2), 181-191.

Laurin, G. V., Ding, J., Disney, M., Bartholomeus, H., Herold, M., Papale, D., & Valentini, R. (2019). Tree height in tropical forest as measured by different ground, proximal, and remote sensing instruments, and impacts on above ground biomass estimates. *International Journal of Applied Earth Observation and Geoinformation*, *82*, 101899.

Li, L., Chen, J., Mu, X., Li, W., Yan, G., Xie, D., & Zhang, W. (2020). Quantifying Understory and Overstory Vegetation Cover Using UAV-Based RGB Imagery in Forest Plantation. *Remote Sensing*, *12*(2), 298.

Li, Z., & Guo, X. (2016). Remote sensing of terrestrial non-photosynthetic vegetation using hyperspectral, multispectral, SAR, and LiDAR data. Progress in Physical Geography, 40(2), 276-304.

Librán-Embid, F., Klaus, F., Tscharntke, T., & Grass, I. (2020). Unmanned aerial vehicles for biodiversity-friendly agricultural landscapes-A systematic review. *Science of The Total Environment,* 139204.

Lomolino, M. V. (2000). Ecology's most general, yet protean 1 pattern: the species-area relationship. *Journal of Biogeography*, *27*(1), 17–26. https://doi.org/10.1046/j.1365-2699.2000.00377.x

Ma, Q., Su, Y., & Guo, Q. (2017). Comparison of canopy cover estimations from airborne LiDAR, aerial imagery, and satellite imagery. *Ieee Journal of Selected Topics in Applied Earth Observations and Remote Sensing*, *10*(9), 4225–4236.

Maas, B., Clough, Y., & Tscharntke, T. (2013). Bats and birds increase crop yield in tropical agroforestry landscapes. *Ecology Letters*, *16*(12), 1480–1487. https://doi.org/10.1111/ele.12194

Mahiga, S. N., Webala, P., Mware, M. J., & Ndang'Ang'A, P. K. (2019). Influence of Land-Use Type on Forest Bird Community Composition in Mount Kenya Forest. *International Journal of Ecology*, *2019*.

Meylan, L., Gary, C., Allinne, C., Ortiz, J., Jackson, L., & Rapidel, B. (2017). Evaluating the effect of shade trees on provision of ecosystem services in intensively managed coffee plantations. *Agriculture, ecosystems & environment*, *245*, 32-42.

Miller, E., Dandois, J. P., Detto, M., & Hall, J. S. (2017). Drones as a tool for monoculture plantation assessment in the steepland tropics. *Forests*, *8*(5), 1–14. https://doi.org/10.3390/f8050168

Mitchell, K. (2010). Quantitative Analysis by the Point-Centered Quarter Method. *ArXiv Preprint*, *arXiv:1010*, 1–56. Retrieved from http://arxiv.org/abs/1010.3303

Naidoo, R. (2004). Species richness and community composition of songbirds in a tropical forest-agricultural landscape. *Animal Conservation*, *7*(1), 93-105.

Nair, P. R. (1985). Classification of agroforestry systems. *Agroforestry systems*, *3*(2), 97-128.

Nair, P. K. R., Nair, V. D., Kumar, B. M., & Showalter, J. M. (2010). Carbon Sequestration in Agroforestry Systems. In *Advances in agronomy* (Vol. 108, pp. 237–307). https://doi.org/10.1016/S0065-2113(10)08005-3

Narango, D. L., Tallamy, D. W., Snyder, K. J., & Rice, R. A. (2019). Canopy tree preference by insectivorous birds in shade-coffee farms: Implications for migratory bird conservation. *Biotropica*, *51*(3), 387-398.

Neita, J. C., & Escobar, F. (2012). The potential value of agroforestry to dung beetle diversity in the wet tropical forests of the Pacific lowlands of Colombia. *Agroforestry Systems*, *85*(1), 121–131. https://doi.org/10.1007/s10457-011-9445-9

Noordermeer, L., Bollandsås, O. M., Ørka, H. O., Næsset, E., & Gobakken, T. (2019). Comparing the accuracies of forest attributes predicted from airborne laser scanning and digital aerial photogrammetry in operational forest inventories. *Remote Sensing of Environment*, *226*, 26-37.

Oborne, M. Mission Planner Home website. Available: http://planner.ardupilot.com. [Accessed April 6, 2019]

Orozco, G. V., Mercedes, C., Espinosa, O., Carlos, J., Salazar, S., Fabián, C., & Pantoja, L. (2012). Carbon storage in agroforestry arrangements associated with coffee (Coffea arabica) in the south of Colombia, 213–221.

Ota, T., Ogawa, M., Mizoue, N., Fukumoto, K., & Yoshida, S. (2017). Forest structure estimation from a UAV-based photogrammetric point cloud in managed temperate coniferous forests. *Forests*, *8*(9), 343.

Packalén, P., & Maltamo, M. (2007). The k-MSN method for the prediction of species-specific stand attributes using airborne laser scanning and aerial photographs. *Remote sensing of Environment*, *109*(3), 328-341.

Panagiotidis, D., Abdollahnejad, A., Surový, P., & Chiteculo, V. (2017). Determining tree height and crown diameter from high-resolution UAV imagery. *International Journal of Remote Sensing*, *38*(8–10), 2392–2410. https://doi.org/10.1080/01431161.2016.1264028

Paneque-Gálvez, J., McCall, M., Napoletano, B., Wich, S., & Koh, L. (2014). Small drones for community-based forest monitoring: An assessment of their feasibility and potential in

tropical areas. *Forests*, *5*(6), 1481-1507.

Parisi, F., Di Febbraro, M., Lombardi, F., Biscaccianti, A. B., Campanaro, A., Tognetti, R., & Marchetti, M. (2019). Relationships between stand structural attributes and saproxylic beetle abundance in a Mediterranean broadleaved mixed forest. *Forest Ecology and Management*, *432*(July 2018), 957–966. https://doi.org/10.1016/j.foreco.2018.10.040

Pauli, N., Barrios, E., Conacher, A. J., & Oberthür, T. (2011). Soil macrofauna in agricultural landscapes dominated by the Quesungual Slash-and-Mulch Agroforestry System, western Honduras. *Applied Soil Ecology*, *47*(2), 119–132. https://doi.org/10.1016/j.apsoil.2010.11.005

Pauli, N., Oberthür, T., Barrios, E., & Conacher, A. J. (2009). Fine-scale spatial and temporal variation in earthworm surface casting activity in agroforestry fields, western Honduras. *Pedobiologia*, *53*(2), 127–139. https://doi.org/10.1016/j.pedobi.2009.08.001

Pereira, H. M., Ferrier, S., Walters, M., Geller, G. N., Jongman, R. H. G., Scholes, R. J., ... & Coops, N. C. (2013). Essential biodiversity variables. *Science*, *339*(6117), 277-278.

Perfecto, I., Vandermeer, J. H., Bautista, G. L., Nunñez, G. I., Greenberg, R., Bichier, P., & Langridge, S. (2004). Greater predation in shaded coffee farms: the role of resident neotropical birds. *Ecology*, *85*(10), 2677-2681.

Petit-Aldana, J., Rahman, M. M., Parraguirre-Lezama, C., Infante-Cruz, A., & Romero-Arenas, O. (2019). Litter Decomposition Process in Coffee Agroforestry Systems. *Journal of forest and environmental science*, *35*(2), 121-139.

Philpott, S. M., & Bichier, P. (2012). Effects of shade tree removal on birds in coffee agroecosystems in Chiapas, Mexico. *Agriculture, ecosystems & environment*, *149*, 171-180.

Pretzsch, H. (2014). Canopy space filling and tree crown morphology in mixed-species stands compared with monocultures. *Forest Ecology and Management*, *327*, 251–264. https://doi.org/10.1016/j.foreco.2014.04.027

Proença, V., Martin, L. J., Pereira, H. M., Fernandez, M., McRae, L., Belnap, J., ... & Honrado, J. P. (2017). Global biodiversity monitoring: from data sources to essential biodiversity variables. *Biological Conservation*, *213*, 256-263.

Proulx, R., Rheault, G., Bonin, L., Roca, I. T., Martin, C. A., Desrochers, L., & Seiferling, I. (2015). How much biomass do plant communities pack per unit volume?. *PeerJ*, *3*, e849.

Puliti, S., Ørka, H. O., Gobakken, T., & Næsset, E. (2015). Inventory of small forest areas using an unmanned aerial system. *Remote Sensing*, *7*(8), 9632–9654. https://doi.org/10.3390/rs70809632

Puliti, S., Solberg, S., & Granhus, A. (2019). Use of uav photogrammetric data for estimation of biophysical properties in forest stands under regeneration. *Remote Sensing*, *11*(3), 233.

Rahlf, J., Breidenbach, J., Solberg, S., Næsset, E., & Astrup, R. (2017). Digital aerial photogrammetry can efficiently support large-area forest inventories in Norway. *Forestry: An International Journal of Forest Research*, *90*(5), 710-718.

Roşca, S., Suomalainen, J., Bartholomeus, H., & Herold, M. (2018). Comparing terrestrial laser scanning and unmanned aerial vehicle structure from motion to assess top of canopy structure in tropical forests. *Interface focus*, *8*(2), 20170038.

Rutten, G., Ensslin, A., Hemp, A., & Fischer, M. (2015). Vertical and horizontal vegetation structure across natural and modified habitat types at Mount Kilimanjaro. *PLoS ONE*, *10*(9), 1–15. https://doi.org/10.1371/journal.pone.0138822

Saarinen, N., Vastaranta, M., Näsi, R., Rosnell, T., Hakala, T., Honkavaara, E., ... & Ribeiro, E.

(2018). Assessing Biodiversity in Boreal Forests with UAV-Based Photogrammetric Point Clouds and Hyperspectral Imaging. *Remote Sensing*, *10*(2), 338. https://doi.org/10.3390/rs10020338

Seidel, D., Fleck, S., Leuschner, C., & Hammett, T. (2011). Review of ground-based methods to measure the distribution of biomass in forest canopies. *Annals of Forest Science*, *68*(2), 225-244.

Segura, M., Kanninen, M., & Suárez, D. (2006). Allometric models for estimating aboveground biomass of shade trees and coffee bushes grown together. *Agroforestry Systems*, *68*(2), 143–150. https://doi.org/10.1007/s10457-006-9005-x

Siles, P., Harmand, J. M., & Vaast, P. (2010). Effects of Inga densiflora on the microclimate of coffee (Coffea arabica L.) and overall biomass under optimal growing conditions in Costa Rica. *Agroforestry systems*, *78*(3), 269-286.

Somarriba, E., Cerda, R., Orozco, L., Cifuentes, M., Dávila, H., Espin, T., … Rica, C. (2013). Carbon stocks and cocoa yields in agroforestry systems of Central America. *Agriculture, Ecosystems and Environment*, *173*, 46–57. https://doi.org/10.1016/j.agee.2013.04.013

Schroth, G., & Harvey, C. A. (2007). Biodiversity conservation in cocoa production landscapes: An overview. *Biodiversity and Conservation*, *16*(8), 2237–2244. https://doi.org/10.1007/s10531-007-9195-1

Steffan-Dewenter, I. (2003). Importance of Habitat Area and Landscape Context for Species Richness of Bees and Wasps in Fragmented Orchard Meadows. *Conservation Biology*, *17*(4), 1036–1044. https://doi.org/10.1046/j.1523-1739.2003.01575.x

Stenchly, K., Clough, Y., & Tscharntke, T. (2012). Spider species richness in cocoa agroforestry systems, comparing vertical strata, local management and distance to forest. *Agriculture,*

Ecosystems and Environment, 149, 189–194. https://doi.org/10.1016/j.agee.2011.03.021

Swallow, B., Boffa, J. M., & Scherr, S. J. (2006). The potential for agroforestry to contribute to the conservation and enhancement of landscape biodiversity. World agroforestry into the future. World Agroforestry Centre (ICRAF), Nairobi, 95-101.

Swinfield, T., Lindsell, J. A., Williams, J. V., Harrison, R. D., Gemita, E., Schönlieb, C. B., & Coomes, D. A. (2019). Accurate measurement of tropical forest canopy heights and aboveground carbon using structure from motion. *Remote Sensing*, *11*(8), 928.

Ullman, S. (1979). The interpretation of structure from motion. *Proceedings of the Royal Society of London. Series B. Biological Sciences*, *203*(1153), 405-426.

van Ewijk, K. Y., Treitz, P. M., & Scott, N. A. (2011). Characterizing forest succession in Central Ontario using LiDAR-derived indices. *Photogrammetric Engineering & Remote Sensing*, *77*(3), 261-269.

Waldron, A., Garrity, D., Malhi, Y., Girardin, C., Miller, D. C., & Seddon, N. (2017). Agroforestry Can Enhance Food Security While Meeting Other Sustainable Development Goals. *Tropical Conservation Science*, *10*, 1–6. https://doi.org/10.1177/1940082917720667

Wallace, L., Lucieer, A., Malenovský, Z., Turner, D., & Vopěnka, P. (2016). Assessment of forest structure using two UAV techniques: A comparison of airborne laser scanning and structure from motion (SfM) point clouds. *Forests*, *7*(3), 62.

Wanger, T. C., Saro, A., Iskandar, D. T., Brook, B. W., Sodhi, N. S., Clough, Y., & Tscharntke, T. (2009). Conservation value of cacao agroforestry for amphibians and reptiles in South-East Asia: Combining correlative models with follow-up field experiments. *Journal of Applied Ecology*, *46*(4), 823–832. https://doi.org/10.1111/j.1365-2664.2009.01663.x

Warde, W., & Petranka, J. W. (1981). A Correction Factor Table for Missing Point-Center Quarter

Data Author. *Ecology*, *62*(2), 491–494.

Wich, S. A., & Koh, L. P. (2018). Conservation drones: Mapping and monitoring biodiversity. Oxford University Press.

Williams-Guillén, K., McCann, C., Martínez Sánchez, J. C., & Koontz, F. (2006). Resource availability and habitat use by mantled howling monkeys in a Nicaraguan coffee plantation: Can agroforests serve as core habitat for a forest mammal? *Animal Conservation*, *9*(3), 331–338. https://doi.org/10.1111/j.1469-1795.2006.00042.x

Wulder, M. A., Hall, R. J., Coops, N. C., & Franklin, S. E. (2004). High spatial resolution remotely sensed data for ecosystem characterization. *BioScience*, *54*(6), 511-521.

Zahawi, R. A., Dandois, J. P., Holl, K. D., Nadwodny, D., Reid, J. L., & Ellis, E. C. (2015). Using lightweight unmanned aerial vehicles to monitor tropical forest recovery. *Biological Conservation*, *186*, 287-295. https://doi.org/10.1016/j.biocon.2015.03.031

Zhang, D., Liu, J., Ni, W., Sun, G., Zhang, Z., Liu, Q., & Wang, Q. (2019). Estimation of Forest Leaf Area Index Using Height and Canopy Cover Information Extracted From Unmanned Aerial Vehicle Stereo Imagery. *IEEE Journal of Selected Topics in Applied Earth Observations and Remote Sensing*, *12*(2), 471-481.

Appendices

Appendix A

Application of PCQM in AFS and forest plots.

Note. The images show procedures to measurements and recording of distances between points, to the nearest neighbors, D_{130} , and height.

Appendix B

Picture taking of hemispheric photographs.

Note. On the bottom left, positions of hemispherical photographs inside each plot are marked with circles. Top left shows an example of a photograph taken in this study inside a cacao crop. Camera accomodation to take the pictures at 1 m of height is presented on the right.

Appendix C

Example of takeoff and retrieval procedure using the UAV mapper.

Note: Upper row shows the takeoff position, against the wind to gain lift and thrust. Bottom row shows the use of parachute during landing. The home site for each flight was an area without dense vegetation or buildings because of the way to takeoff of a fixed wing drone. The landing of each flight was made in the opposite direction to the wind and always assisted with the remote control. In order to prevent collisions, we sometimes use the parachute, which can help a lot with landing in mountainous areas where large trees are present. Before each flight with the UAV, we had to do the compass calibration with the tip facing north while rotating around its three axes for approximately one minute. Altitude of flights varies between 150 and 200 m over the home and this only depended on the site topography and the associated risks.

Appendix D

Orthoimages from two neighboring farms with different intensity of management for AFS with cacao.

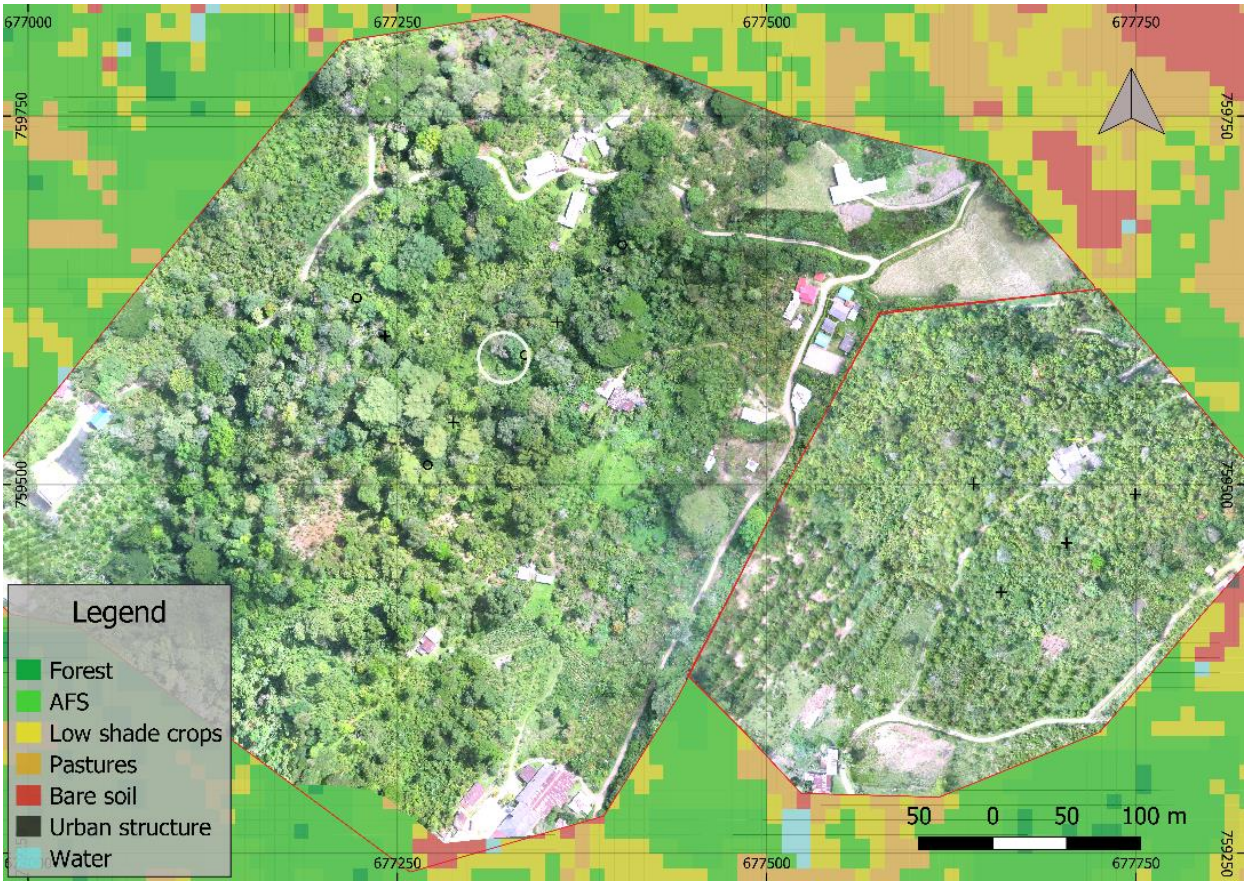

Note. The background is a land cover classification constructed with multispectral images of Sentinel-2 satellite. This is a zoom in *Figure 1*. Included into the document.

Appendix E

Orthoimage of a riparian farm with high shade AFS with cacao.

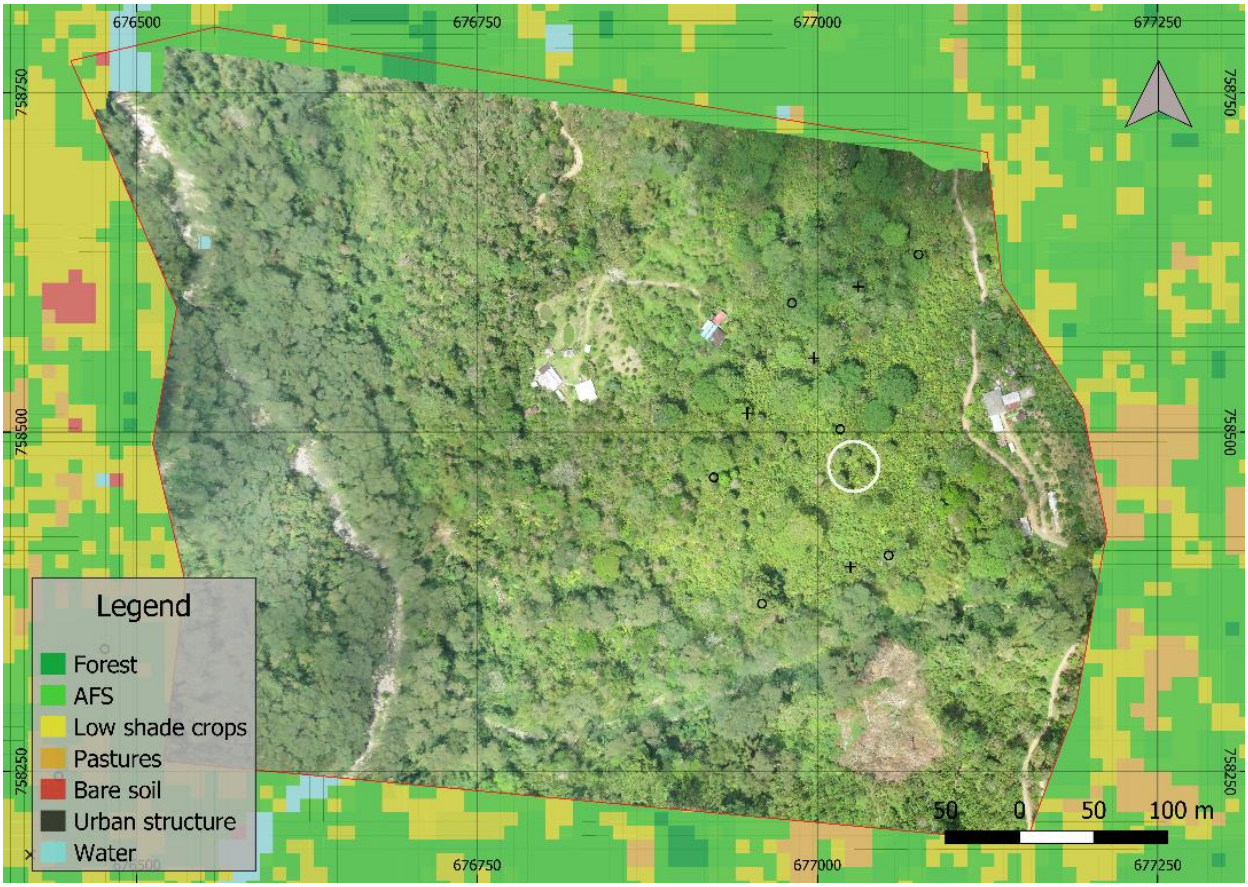

Note. on the left of the image we see the stream of *Las Cruces.* Again, this is the zoom in *Figure 1.* (see body of the document)

Appendix F

Two orthoimages of four neighbor farms.

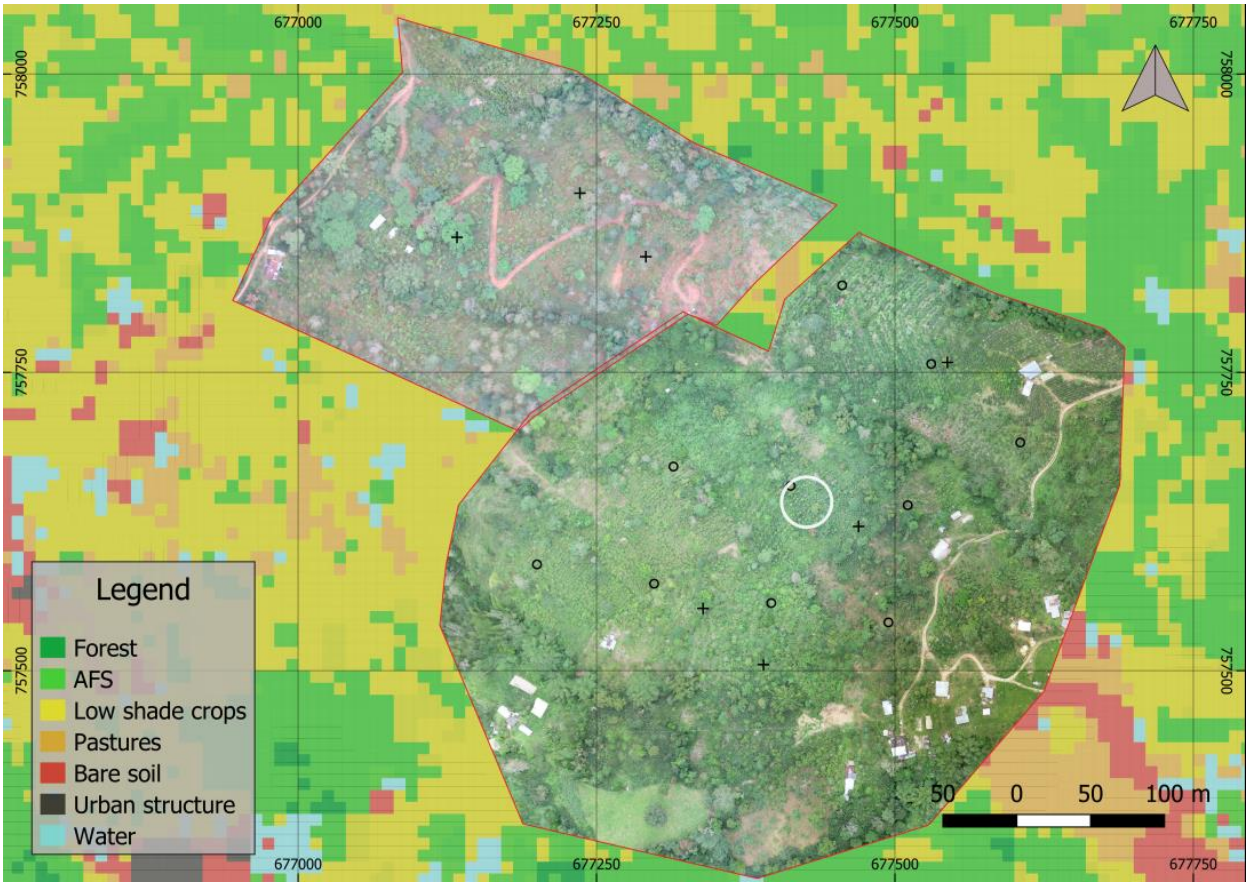

Note. The orthomosaics show differences in light intensity due different environmental conditions at time flights.

Appendix G

Orthoimage of a riparian farm and little village inside Las Cruces micro-watershed.

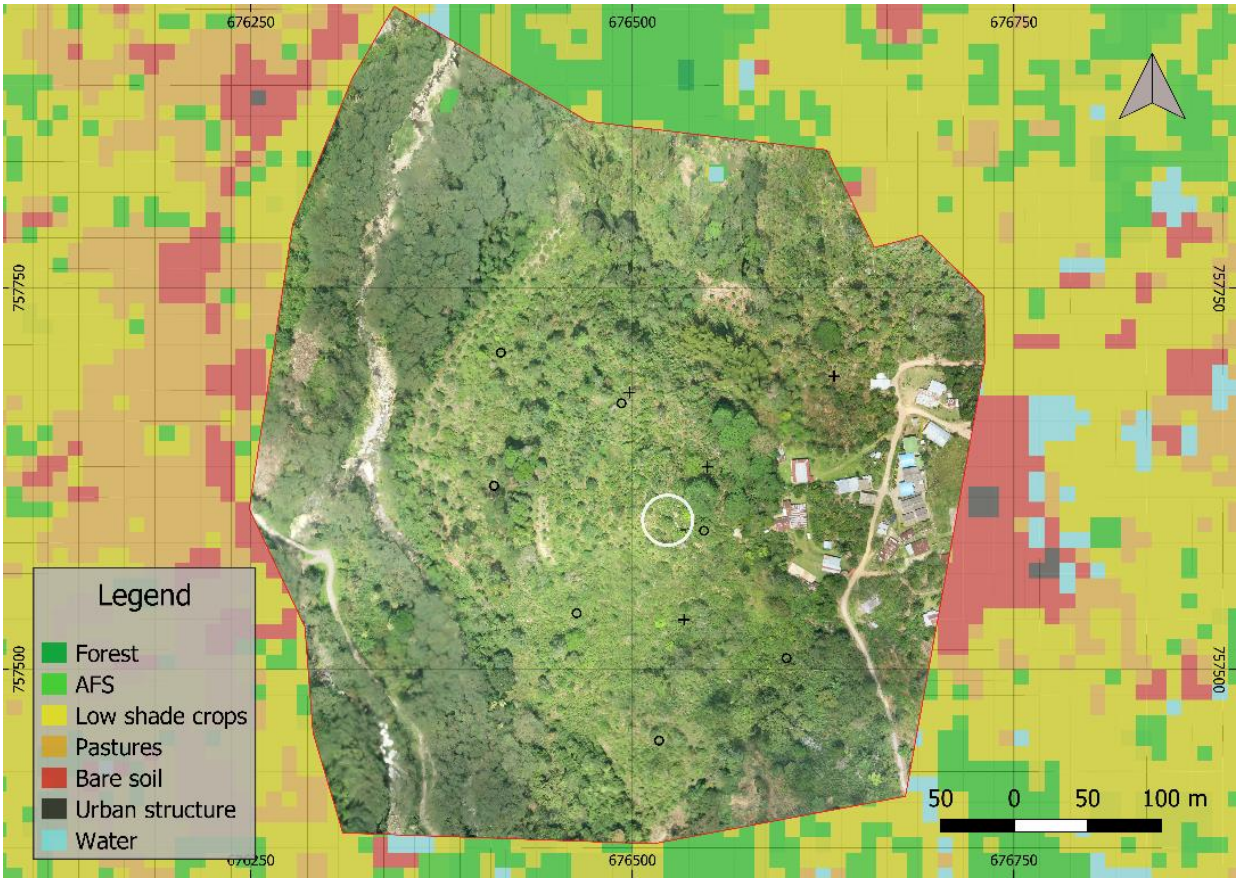

Appendix H

Orthoimage of a farm which has multiple productive systems, as AFS with cacao, coffee, and fish.

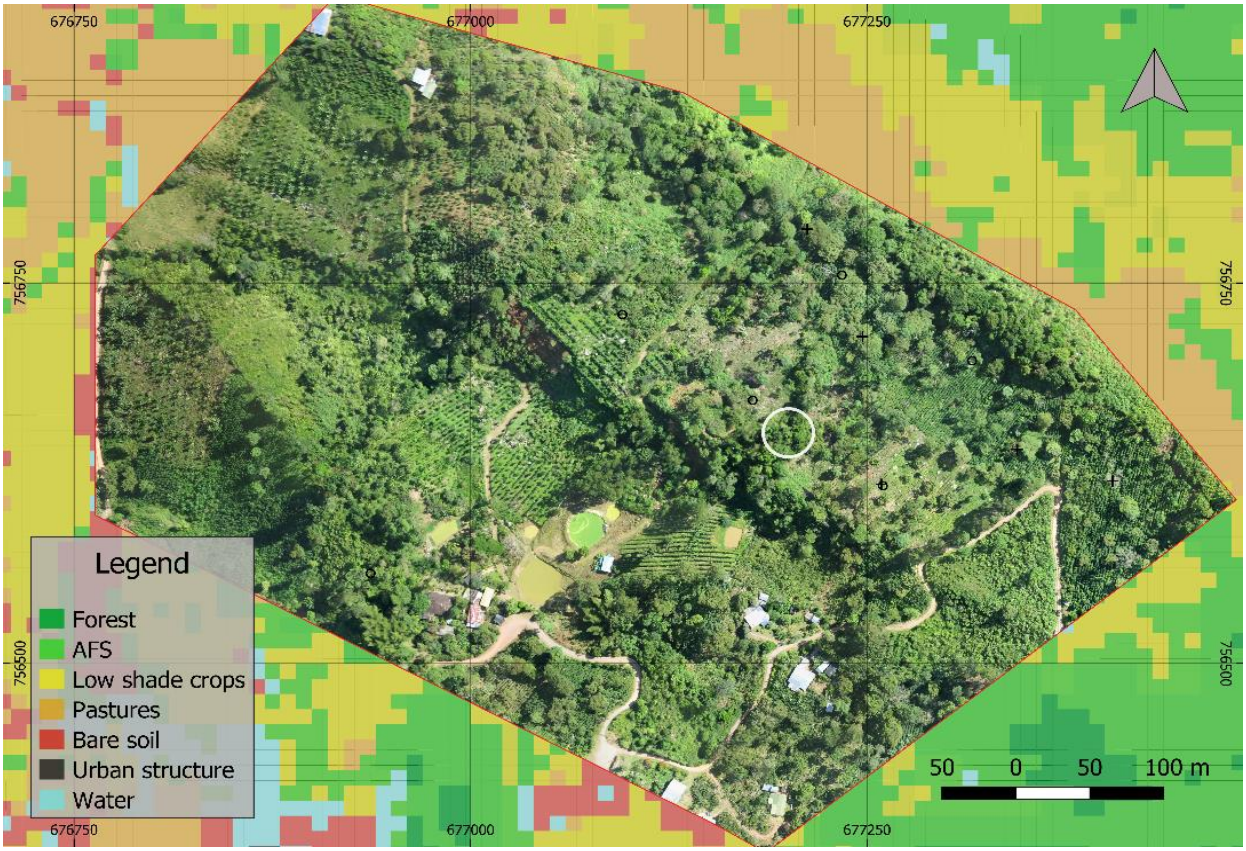

Appendix I

Two orthoimages of three different farms.

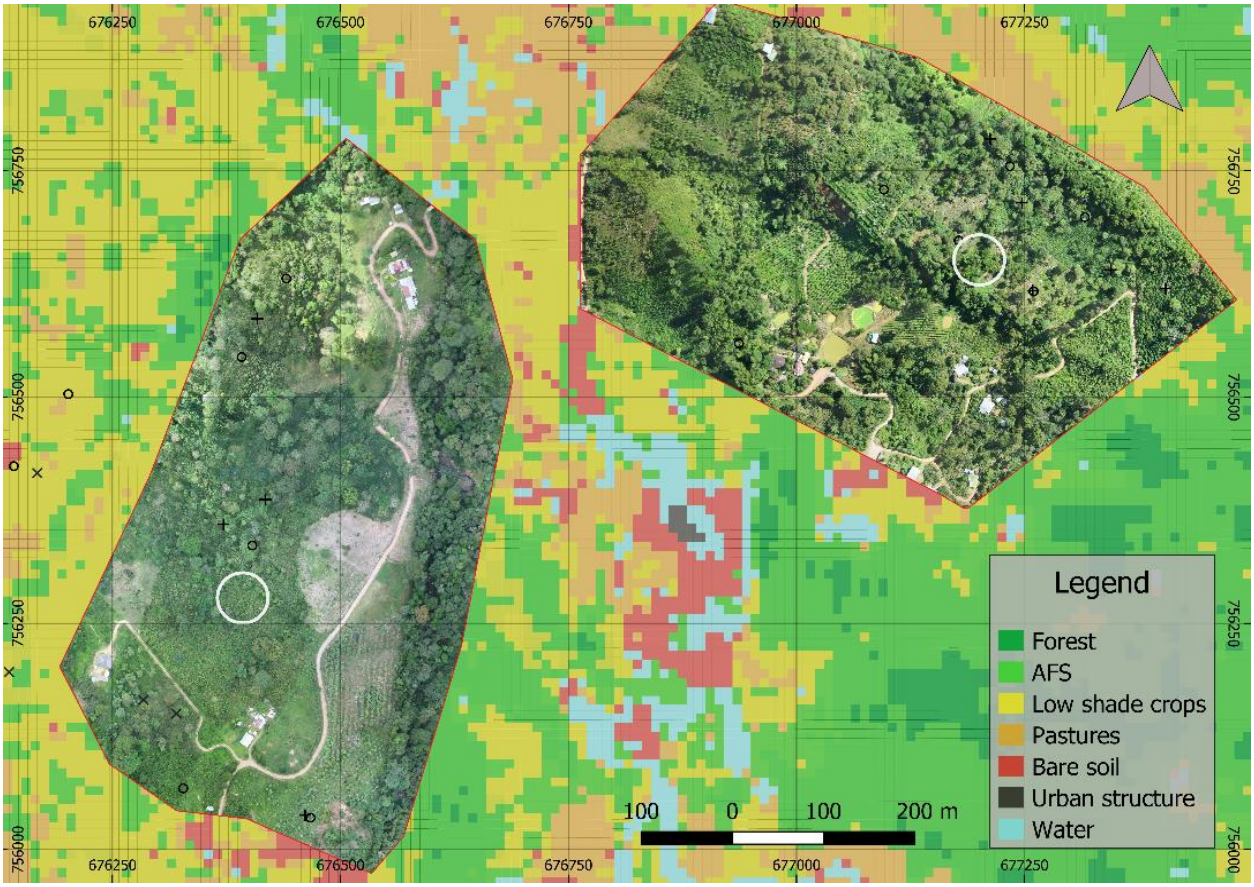

Note. differences in light conditions are observed even inside one scene due the presence and fast movement of clouds.

Appendix J

Orthoimage of the farm to which forest belongs.

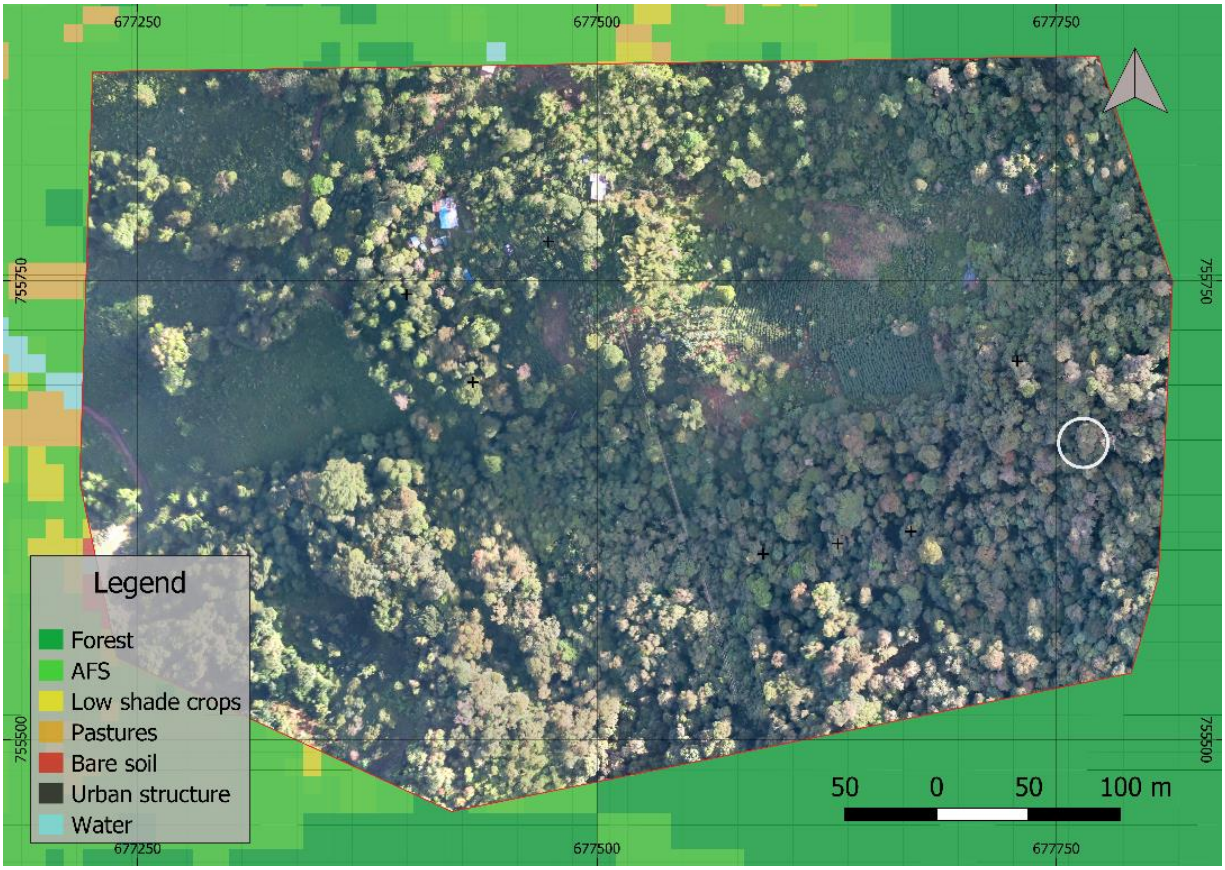

Note. the forest is located to the south-east region of orthomosaic.